

One-year, regional-scale simulation of  $^{137}\text{Cs}$  radioactivity in the ocean

D. Tsumune et al.

# One-year, regional-scale simulation of $^{137}\text{Cs}$ radioactivity in the ocean following the Fukushima Daiichi Nuclear Power Plant accident

D. Tsumune<sup>1</sup>, T. Tsubono<sup>1</sup>, M. Aoyama<sup>2</sup>, M. Uematsu<sup>3</sup>, K. Misumi<sup>1</sup>, Y. Maeda<sup>1</sup>, Y. Yoshida<sup>1</sup>, and H. Hayami<sup>1</sup>

<sup>1</sup>Environmental Science Research Laboratory, Central Research Institute of Electric Power Industry, Chiba, Japan

<sup>2</sup>Meteorological Research Institute, Tsukuba, Japan

<sup>3</sup>Ocean Research Institute, University of Tokyo, Tokyo, Japan

Received: 30 December 2012 – Accepted: 13 March 2013 – Published: 3 April 2013

Correspondence to: D. Tsumune (tsumune@criepi.denken.or.jp)

Published by Copernicus Publications on behalf of the European Geosciences Union.

Title Page

Abstract

Introduction

Conclusions

References

Tables

Figures

⏪

⏩

◀

▶

Back

Close

Full Screen / Esc

Printer-friendly Version

Interactive Discussion

## Abstract

A series of accidents at the Fukushima Dai-ichi Nuclear Power Plant following the earthquake and tsunami of 11 March 2011 resulted in the release of radioactive materials to the ocean by two major pathways, direct release from the accident site and atmospheric deposition. A 1 yr, regional-scale simulation of  $^{137}\text{Cs}$  activity in the ocean offshore of Fukushima was carried out, the sources of radioactivity being direct release, atmospheric deposition, and the inflow of  $^{137}\text{Cs}$  deposited on the ocean by atmospheric deposition outside the domain of the model.

Direct releases of  $^{131}\text{I}$ ,  $^{134}\text{Cs}$ , and  $^{137}\text{Cs}$  were estimated for 1 yr after the accident by comparing simulated results and measured activities. The estimated total amounts of directly released  $^{131}\text{I}$ ,  $^{134}\text{Cs}$ , and  $^{137}\text{Cs}$  were  $11.1 \pm 2.2$  PBq,  $3.5 \pm 0.7$  PBq, and  $3.6 \pm 0.7$  PBq, respectively. The contributions of each source were estimated by analysis of  $^{131}\text{I}/^{137}\text{Cs}$  and  $^{134}\text{Cs}/^{137}\text{Cs}$  activity ratios and comparisons between simulated results and measured activities of  $^{137}\text{Cs}$ . Simulated  $^{137}\text{Cs}$  activities attributable to direct release were in good agreement with measured activities close to the accident site, a result that implies that the estimated direct release rate was reasonable, while simulated  $^{137}\text{Cs}$  activities attributable to atmospheric deposition were low compared to measured activities. The rate of atmospheric deposition onto the ocean was underestimated because of a lack of measurements of deposition onto the ocean when atmospheric deposition rates were being estimated. Measured  $^{137}\text{Cs}$  activities attributable to atmospheric deposition helped to improve the accuracy of simulated atmospheric deposition rates. Simulated  $^{137}\text{Cs}$  activities attributable to the inflow of  $^{137}\text{Cs}$  deposited onto the ocean outside the domain of the model were in good agreement with measured activities in the open ocean within the model domain after June 2012. The contribution of inflow increased with time and was dominant (more than 99%) by the end of February 2012. The activity of directly released  $^{137}\text{Cs}$ , however, decreased exponentially with time and was detectable only in the coastal zone by the end of February 2012.

### One-year, regional-scale simulation of $^{137}\text{Cs}$ radioactivity in the ocean

D. Tsumune et al.

Title Page

Abstract

Introduction

Conclusions

References

Tables

Figures

◀

▶

◀

▶

Back

Close

Full Screen / Esc

Printer-friendly Version

Interactive Discussion



## 1 Introduction

Radioactive materials were released to the environment from the Tokyo Electric Power Company (TEPCO) Fukushima Dai-ichi Nuclear Power Plant (hereafter 1F NPP) as a result of reactor accidents caused by a total loss of electric power after the Tohoku earthquake and tsunami on 11 March 2011. Radioactive materials were emitted into the atmosphere and transferred to the land and ocean through wet and dry deposition. In addition, highly contaminated water was directly released to the ocean. Radioactive materials were released to the ocean by two major pathways, direct release from the site of the 1F NPP accident and atmospheric deposition.

On 21 March 2011 TEPCO started measuring the activities of radioisotopes in sea-water adjacent to the discharge canal for reactors 5 and 6 (5–6 discharge canal) on the north side of the 1F NPP site and the discharge canal for reactors 1–4 (south discharge canal) on the south side of the 1F NPP site, the north discharge canal at the Fukushima Daini Nuclear Power Plant (2F NPP) site (10 km south of the 1F NPP site), and offshore of Iwasawa (16 km south of the 1F NPP site) (TEPCO, 2012a). The Ministry of Education, Culture, Sports, Science & Technology of Japan (MEXT) measured the activities of  $^{131}\text{I}$ ,  $^{134}\text{Cs}$ , and  $^{137}\text{Cs}$  at eight sites 30 km offshore of the 1F NPP from 23 March to 8 May 2011 (MEXT, 2012). After May 8, TEPCO increased the number of measurement sites within that original sampling area, and MEXT also increased the number of its sampling sites and extended them over a wider area off the Fukushima coast. The cruise of the research vessel *Ka'imikai-o-Kanaloa* (KOK) covered that wider area during 4–18 June 2011 (Buesseler et al., 2012). The measured  $^{137}\text{Cs}$  activities at most sites decreased exponentially with time, but by the end of February 2012 they were still higher than the background activity due to global fallout ( $1\text{--}2\text{ Bq m}^{-3}$ ; Historical Artificial Radionuclides in the Pacific Ocean and its Marginal Seas (HAM) database; Aoyama and Hirose, 2004 and extended). Basin-scale measurements were made by 17 Voluntary Observing Ships (VOS) and several research vessels in the North Pacific for 1 yr after the accident (Honda et al., 2012; Aoyama et al., 2012a, b, c, 2013a, b).

### One-year, regional-scale simulation of $^{137}\text{Cs}$ radioactivity in the ocean

D. Tsumune et al.

Title Page

Abstract

Introduction

Conclusions

References

Tables

Figures

◀

▶

◀

▶

Back

Close

Full Screen / Esc

Printer-friendly Version

Interactive Discussion

Aoyama et al. (2012c, 2013b) used atmospheric and oceanic numerical simulations to estimate the contributions to the contamination from direct release and atmospheric deposition in the North Pacific. Here we focus on the estimation of contributions to contamination from direct release and atmospheric deposition on a regional scale.

Oceanic numerical simulation is useful for estimating the rates of direct release and for representing and predicting the behavior of radioactive materials. Reconstruction of the history of the activities of radioactive materials by numerical simulations is useful for understanding the history and processes of radioactive contamination of oceanic biota (Tateda et al., 2013).

Tsumune et al. (2012) used a regional ocean model simulation to estimate direct release rates until the end of May 2011. In the study, the analysis of  $^{131}\text{I}/^{137}\text{Cs}$  activity ratios indicated that direct releases started on 26 March 2011 and the total amount of  $^{137}\text{Cs}$  activity released was estimated to be  $(3.5 \pm 0.7) \times 10^{15}$  Bq ( $3.5 \pm 0.7$  PBq) by the end of May. Although the model assumed that direct releases were the only sources of radioactivity and atmospheric deposition was ignored, nearshore simulated and measured  $^{137}\text{Cs}$  activities were in good agreement during the first period of the simulation.

Oceanic numerical simulations have been performed at a regional scale along the coast (summarized in Masumoto et al., 2012; Miyazawa et al., 2012a). One way to estimate direct release rates was only by measurements. Numerical simulations have been also used to estimate direct release rates by comparing measurements with simulated results. Inverse methods have been applied to estimate direct release rates. The amount of directly released radioactivity estimated from measured radioactivities only varied much from 0.94 to 27 PBq (Japanese Government, 2011; Kawamura et al., 2011; Bailly du Bois et al., 2012), on the other hand, the amount of directly released radioactivity estimated from the numerical simulations and inverse methods varied from  $3.5 \pm 0.7$  to 5.5–5.9 PBq (Tsumune et al., 2012; Estournel et al., 2012; Miyazawa et al., 2012b). These discrepancies also reflect differences in the estimated durations of the releases and in the analytical methods. We will discuss these differences in Sect. 4.2.

## One-year, regional-scale simulation of $^{137}\text{Cs}$ radioactivity in the ocean

D. Tsumune et al.

[Title Page](#)[Abstract](#)[Introduction](#)[Conclusions](#)[References](#)[Tables](#)[Figures](#)[⏪](#)[⏩](#)[◀](#)[▶](#)[Back](#)[Close](#)[Full Screen / Esc](#)[Printer-friendly Version](#)[Interactive Discussion](#)

The contribution of atmospheric deposition to oceanic contamination is still unclear. The duration of the regional simulations was several months.

We expanded the model domain of our previous simulation (Tsumune et al., 2012) and extended the period of simulation for 1 yr, until the end of February 2012. Unlike the previous simulations that took into account only direct releases of radioactivity, the expanded model also estimated the contribution of atmospheric deposition to oceanic contamination.

## 2 Materials and methods

### 2.1 Monitoring data

On 21 March 2011 TEPCO began measuring the radioactivity of seawater adjacent to the mouth of the discharge canal for reactors 5 and 6 (5–6 discharge canal) on the north side of the 1F NPP site, the discharge canal for reactors 1–4 (south discharge canal) on the south of the 1F NPP site, the north discharge canal at the Fukushima Daini Nuclear Power Plant (2F NPP) site (10 km south of the 1F NPP site), and a site offshore of Iwasawa (16 km south of the 1F NPP site) (TEPCO, 2012a). MEXT measured the activities of  $^{131}\text{I}$ ,  $^{134}\text{Cs}$ , and  $^{137}\text{Cs}$  at eight sites 30 km offshore of Fukushima Prefecture from 23 March to 8 May (MEXT, 2012). TEPCO and MEXT published the data without error bars on their website. There was a systematic 33 % error in the data. TEPCO increased the number of measurement sites within 30 km of the coast (Fig. S1). MEXT increased the number of its sampling sites and extended them over a wider area during 23–27 August 2011 and from 30 November to 2 December 2011 (MEXT, 2012). The cruise of the research vessel (R/V) *Ka'imikai-o-Kanaloa* (KOK) covered that wider area off the Fukushima coast during 4–18 June 2011 (Buesseler et al., 2012).

**BGD**

10, 6259–6314, 2013

**One-year,  
regional-scale  
simulation of  $^{137}\text{Cs}$   
radioactivity in the  
ocean**

D. Tsumune et al.

Title Page

Abstract

Introduction

Conclusions

References

Tables

Figures

◀

▶

◀

▶

Back

Close

Full Screen / Esc

Printer-friendly Version

Interactive Discussion

## 2.2 Atmospheric model

We employed the Comprehensive Air Quality Model with eXtensions (CAMx; ENVIRON, 2009) to simulate atmospheric activities and the deposition of  $^{137}\text{Cs}$  released from the 1F NPP reactors. CAMx is a three-dimensional air quality model formulated using terrain-following coordinates; it includes detailed sub-models that simulate advection and dispersion, chemical reactions, aerosol dynamics, cloud processes, and dry and wet deposition. We utilized a simple user-defined chemistry mechanism with radioactive decay of  $^{137}\text{Cs}$ . The sub-model assumed that  $^{137}\text{Cs}$  was present in particles with a mean diameter of  $0.31\ \mu\text{m}$ . The activity of  $^{137}\text{Cs}$  was taken from Terada et al. (2012). The total estimated activity was  $9.0\ \text{PBq}$  from 11 March to 1 April 2011.

CAMx was driven by the Weather Research and Forecasting model version V3.2.1 (WRF; Skamarock et al., 2008). The horizontal domain of WRF is  $960 \times 1010\ \text{km}$  in the zonal and meridional directions with a resolution of  $5\ \text{km}$ . The vertical domain, from the surface to  $100\ \text{hPa}$ , is divided into 30 layers in the  $\sigma$  coordinate system. The height of the lowest layer is about  $52\ \text{m}$  in the standard atmosphere. The initial and boundary fields were produced from the operational mesoscale numerical weather analysis by the Japan Meteorological Agency (MANAL; every  $5\ \text{km}$  and  $3\ \text{h}$ ). The wind fields were nudged throughout the domain and duration of the simulation. We also used the  $30\ \text{s}$  land-use data of the United States Geological Survey and the hourly sea surface temperature data from the National Center for Environmental Prediction/National Oceanic and Atmospheric Administration real-time, global, sea surface temperature (RTG\_SST\_HR) analysis. WRF ran for 4 March to 1 April 2011, UTC.

The CAMx domain is  $900 \times 950\ \text{km}$  inside the WRF domain and includes 14 vertical layers, the uppermost of the 30 layers in the WRF having been collapsed. The CAMx simulation ran from 11 March to 1 April 2011, UTC. Hourly activities and depositions were stored for validation and analysis.

BGD

10, 6259–6314, 2013

### One-year, regional-scale simulation of $^{137}\text{Cs}$ radioactivity in the ocean

D. Tsumune et al.

Title Page

Abstract

Introduction

Conclusions

References

Tables

Figures

◀

▶

◀

▶

Back

Close

Full Screen / Esc

Printer-friendly Version

Interactive Discussion

## 2.3 Oceanic model

We employed the Regional Ocean Modeling System (ROMS; Shchepetkin and McWilliams, 2005) to simulate the behavior of  $^{137}\text{Cs}$  released from the 1F NPP reactors off Fukushima. The ROMS is a three-dimensional Boussinesq free-surface ocean circulation model formulated using terrain-following coordinates. We expanded the model domain and extended the simulated period (Tsumune et al., 2012) of the previous model.

The model domain in this study covered the oceanic area off Fukushima ( $35^{\circ} 54' \text{N}$ – $40^{\circ} 00' \text{N}$ ,  $139^{\circ} 54' \text{E}$ – $147^{\circ} 00' \text{E}$ ). The horizontal resolution was 1 km in both zonal and meridional directions. The vertical resolution of the  $\sigma$  coordinate was 30 layers. The ocean bottom was set at a depth of 1000 m to reduce the computer resources needed for the simulation. The actual ocean depth reaches more than 1500 m in this region. This domain is larger and deeper than the one used by Tsumune et al. (2012) (Fig. S2). Numerical conditions were similar to those in this previous model. We used a third-order upwind difference for the advection scheme for both momentum and tracers and a fourth-order centered difference scheme for viscosity and diffusivity in the model. The horizontal viscosity and diffusion coefficient were  $5.0 \text{ m}^2 \text{ s}^{-1}$ . The vertical viscosity and diffusion coefficient were obtained by K-profile parameterization (Large et al., 1994). The background value of the vertical viscosity and diffusion coefficient was  $10^{-5} \text{ m}^2 \text{ s}^{-1}$ .

The model was forced at the sea surface by wind stress and heat and freshwater fluxes, the values of which were acquired by a real-time nested simulation system (NuWFAS, Hashimoto et al., 2010) of the WRF, a global spectral model used for numerical weather prediction by the Japan Meteorological Agency (JMA). The horizontal resolution of the system was 5 km in both the zonal and meridional directions. The time step of the output from the real-time simulation system was 1 h, and the duration of the simulation was 1 yr.

During the simulation, horizontal currents, temperature, salinity, and sea surface height along the open boundary were restored to the JCOPE2 reanalysis data

BGD

10, 6259–6314, 2013

### One-year, regional-scale simulation of $^{137}\text{Cs}$ radioactivity in the ocean

D. Tsumune et al.

Title Page

Abstract

Introduction

Conclusions

References

Tables

Figures

◀

▶

◀

▶

Back

Close

Full Screen / Esc

Printer-friendly Version

Interactive Discussion

## One-year, regional-scale simulation of $^{137}\text{Cs}$ radioactivity in the ocean

D. Tsumune et al.

Title Page

Abstract

Introduction

Conclusions

References

Tables

Figures

◀

▶

◀

▶

Back

Close

Full Screen / Esc

Printer-friendly Version

Interactive Discussion

(JCOPE2, Japan Coastal Ocean Prediction Experiment 2, Miyazawa et al., 2009) instead of the Real-time  $1/12^\circ$  Global HYCOM (HYbrid Coordinate Ocean Model) Nowcast/Forecast System results (Chassignet et al., 2006). Temperature and salinity were nudged to the JCOPE2 reanalysis results to represent mesoscale eddies during the simulation period. The nudging parameter was  $1 \text{ d}^{-1}$ . The initial conditions of temperature, salinity, horizontal current velocities, and sea surface height were set by the JCOPE2 reanalysis output. Tidal effects were ignored in this model.

We modeled  $^{137}\text{Cs}$  as a passive tracer, its movement into the ocean interior being controlled by advection and diffusion. We assumed the activity of  $^{137}\text{Cs}$  in seawater to decrease as a result of radioactive decay with a half-life of 30 yr. The effect of decay was negligible during the simulation period of 1 yr, from 1 March 2011 to 29 February 2012.

### 2.4 Inflow from boundary sections

Atmospheric deposition occurred throughout the North Pacific Ocean, but our model domain was too small to represent the effects of atmospheric deposition over such a wide area. Fluxes through boundaries are therefore important for long-term simulation of the effects of atmospheric deposition at a regional scale. One of the simulated  $^{137}\text{Cs}$  activities in the North Pacific (Aoyama et al., 2012c, 2013b) was set as boundary conditions for this model from March 2011 to February 2012.

Aoyama et al. (2012c, 2013b) used a global aerosol transport model referred to as the Model of Aerosol Species IN the Global Atmosphere (MASINGAR mk-2) with an atmospheric general circulation model as a component of the Earth system model of Meteorological Research Institute, MRI-ESM1 (Yukimoto et al., 2011). The model resolutions were set to a TL319 horizontal grid (about  $0.5625^\circ \times 0.5625^\circ$ ) and 40 vertical layers from the ground surface to a height of 0.4 hPa. In this experiment, the horizontal wind fields were assimilated with the six-hourly,  $1.25^\circ \times 1.25^\circ$  data of the Japan Meteorological Agency (JMA) global optimal analysis. Emission scenario of  $^{137}\text{Cs}$  was taken from Terada et al. (2012). The total estimated activity was 9.0 PBq from 11 March to



1 April 2011. And then, the ROMS was employed to simulate the distribution of  $^{137}\text{Cs}$  in the whole North Pacific ( $10^{\circ}\text{S}$ – $60^{\circ}\text{N}$ ,  $110^{\circ}\text{E}$ – $75^{\circ}\text{W}$ ). The horizontal resolution was about 10 km. The vertical resolution of the  $\sigma$  coordinate was 30 layers. They used a third-order upwind difference for the advection scheme for both momentum and tracers and a fourth-order centred difference scheme for viscosity and diffusivity in the model. The horizontal viscosity and diffusion coefficient was  $50\text{m}^2\text{s}^{-1}$ . The vertical viscosity and diffusion coefficient was obtained by K-profile parameterization (Large et al., 1994). The background value of the vertical viscosity and diffusion coefficient was  $10^{-5}\text{m}^2\text{s}^{-1}$ . The model was forced at the sea surface by wind stress and heat and freshwater fluxes by Normal Year Forcing (Large and Yeager, 2004). Direct release rate of  $^{137}\text{Cs}$  from the site of FNPP1 was set in a similar manner in a regional simulation. Background  $^{137}\text{Cs}$  activities due to global fallout from atmospheric nuclear weapons tests before the Fukushima accident were acquired from a global simulation (Tsumune et al., 2011). The simulated background  $^{137}\text{Cs}$  activities of  $1\text{--}3\text{Bqm}^{-3}$  in the North Pacific simulation were set as the initial condition. We set simulated  $^{137}\text{Cs}$  activity by the North Pacific model to the boundary sections of a regional model off Fukushima to simulate the inflow of  $^{137}\text{Cs}$  attributable to atmospheric deposition outside the model domain.

## 2.5 Input sources for $^{137}\text{Cs}$ simulations

The  $^{137}\text{Cs}$  simulations took into account the effects of direct releases and atmospheric deposition. We ignored other sources such as river and groundwater input and sedimentation process in this model to investigate  $^{137}\text{Cs}$  activity in sea water. Figure 1 is a schematic representation of the inputs of  $^{137}\text{Cs}$  from direct releases, atmospheric deposition, and the inflow of  $^{137}\text{Cs}$  attributable to atmospheric deposition outside the model domain and transport through the northern, eastern, and southern boundaries of the model domain. Direct releases accounted for most of the inputs prior to the middle of April 2011 and decreased exponentially with time and atmospheric deposition

## BGD

10, 6259–6314, 2013

### One-year, regional-scale simulation of $^{137}\text{Cs}$ radioactivity in the ocean

D. Tsumune et al.

Title Page

Abstract

Introduction

Conclusions

References

Tables

Figures



Back

Close

Full Screen / Esc

Printer-friendly Version

Interactive Discussion

5 onto the ocean began to occur by early April while the effects of inflow continued for a long time. We compared the simulation with measured  $^{137}\text{Cs}$  activities to investigate the behavior of released  $^{137}\text{Cs}$  and to estimate release rates. Measured  $^{137}\text{Cs}$  activities in the domain of this model reflect inputs from direct releases, atmospheric deposition, and fluxes through boundaries (inflow). Three types of simulations were carried out to elucidate the contributions of the sources of  $^{137}\text{Cs}$ : ALL (Direct release + Atmospheric deposition + Inflow), NO\_INFLOW (Direct release + Atmospheric deposition), and D\_RELEASE (Direct release) (Table 1).

### 3 Results

#### 10 3.1 Direct release rates

Tsumune et al. (2012) used a regional ocean simulation model to estimate direct releases of radioactivity until the end of May 2011. Analysis of  $^{131}\text{I}/^{137}\text{Cs}$  activity ratios indicated that direct releases began on 26 March 2011 (JST). On 26 March the  $^{131}\text{I}/^{137}\text{Cs}$  activity ratio associated with direct releases was 5.7, which is similar to the ratio in a puddle of water in the basement of the 1F NPP reactor 2 turbine building. The  $^{131}\text{I}/^{137}\text{Cs}$  activity ratio associated with atmospheric deposition varied from 0.1 to 10 at 1F NPP, 2F FPP, the Iwasawa coast, and 30 km offshore. These values were estimated from the  $^{131}\text{I}/^{137}\text{Cs}$  activity ratio of soil samples, which were presumed to reflect the effects of atmospheric deposition (Kinoshita et al., 2011).

20 The results of our analysis of  $^{137}\text{Cs}$  activities and  $^{131}\text{I}/^{137}\text{Cs}$  activity ratios suggest that direct releases of  $^{137}\text{Cs}$  from the 1F NPP reactor occurred for 12 days from 26 March to 6 April 2011. The average  $^{137}\text{Cs}$  activity detected near the 1F NPP site was  $1.1 \times 10^7 \text{ Bq m}^{-3}$ . Tsumune et al. (2012) used a simple release scenario to estimate the radioactivity directly released over the entire 12 days. In this scenario, the rate of release of  $^{137}\text{Cs}$  was  $1 \text{ Bqs}^{-1}$  during the 12 days from 26 March to 6 April into the water column of an area simulated by a mesh of grid points adjacent to the 1F

One-year, regional-scale simulation of  $^{137}\text{Cs}$  radioactivity in the ocean

D. Tsumune et al.

Title Page

Abstract

Introduction

Conclusions

References

Tables

Figures

◀

▶

◀

▶

Back

Close

Full Screen / Esc

Printer-friendly Version

Interactive Discussion

## One-year, regional-scale simulation of $^{137}\text{Cs}$ radioactivity in the ocean

D. Tsumune et al.

Title Page

Abstract

Introduction

Conclusions

References

Tables

Figures

◀

▶

◀

▶

Back

Close

Full Screen / Esc

Printer-friendly Version

Interactive Discussion

NPP site. We then calculated a scaling factor between the measured activities and the activities simulated with a constant release rate of  $1 \text{ Bqs}^{-1}$ . We multiplied the simulated  $^{137}\text{Cs}$  activities by the scaling factor so that the average simulated  $^{137}\text{Cs}$  activities in the mesh from 26 March to 6 April were equal to the  $^{137}\text{Cs}$  activities measured at the 5–6 and south discharge canals near the 1F NPP site. The resulting scaling factor,  $2.55 \times 10^9$ , was used to estimate the rate at which  $^{137}\text{Cs}$  activity was directly released from 26 March to 6 April, the estimated rate being  $2.2 \times 10^{14} \text{ Bq day}^{-1}$ . The total activity released by the end of May was estimated to be  $(3.5 \pm 0.7) \times 10^{15} \text{ Bq}$  ( $3.5 \pm 0.7 \text{ PBq}$ ). From 7 to 26 April 2011 the release rate decreased exponentially in a manner similar to the  $^{137}\text{Cs}$  activity. Tsumune et al. (2012) estimated the release rate to be constant after 27 April 2011. In this paper, we used exponential models to describe the releases during each period to improve the agreement between the measured and simulated long-term trend of  $^{137}\text{Cs}$  activity adjacent to the 1F NPP as follows:

26 March–6 April 2011;  $1.1 \times 10^7 \text{ Bqm}^{-3}$  (constant)

7 April–25 April 2011;  $1.1 \times 10^7 e^{(-0.236t)} \text{ Bqm}^{-3}$

26 April–30 June 2011;  $1.2 \times 10^5 e^{(-0.026t)} \text{ Bqm}^{-3}$

1 July 2011–29 February 2012;  $2.3 \times 10^4 e^{(-0.013t)} \text{ Bqm}^{-3}$

where  $t$  is the elapsed time in days since the start of the time interval. Figure 2 shows the  $^{137}\text{Cs}$  activity at the 5–6 and south discharge canals near the 1F NPP site and the exponential curve fit to the data. The measured data were sparse from July to October 2011 because the detection limit of the monitoring by TEPCO and MEXT was higher during that period.

We estimated the rate of direct release of  $^{137}\text{Cs}$  by fitting an exponential function to the measured data near the 1F NPP after 7 April 2011. The estimated total amount of  $^{137}\text{Cs}$  was 3.51 PBq by the end of May (Tsumune et al., 2012) and increased to be 3.55 PBq by the end of February 2012. We were also able to estimate the direct release rates of  $^{131}\text{I}$  and  $^{134}\text{Cs}$  from the activity ratios and half-lives of the isotopes.

## One-year, regional-scale simulation of $^{137}\text{Cs}$ radioactivity in the ocean

D. Tsumune et al.

[Title Page](#)

[Abstract](#)

[Introduction](#)

[Conclusions](#)

[References](#)

[Tables](#)

[Figures](#)

[⏪](#)

[⏩](#)

[◀](#)

[▶](#)

[Back](#)

[Close](#)

[Full Screen / Esc](#)

[Printer-friendly Version](#)

[Interactive Discussion](#)

The  $^{131}\text{I}/^{137}\text{Cs}$  and  $^{134}\text{Cs}/^{137}\text{Cs}$  activity ratios are changed only by the effect of decay and are not changed by transport in seawater (Tsumune et al., 2012). Because the  $^{131}\text{I}/^{137}\text{Cs}$  activity ratio was 5.7 on 26 March 2011 in a puddle of water in the basement of the 1F NPP reactor 2 turbine building, we assumed the  $^{131}\text{I}/^{137}\text{Cs}$  activity ratio in the water directly discharged to the ocean to be 5.7 on 26 March 2011. The ratio decreased with time because the half-life of  $^{131}\text{I}$  (8 d) is very short compared to the 30 yr half-life of  $^{137}\text{Cs}$ . The  $^{134}\text{Cs}/^{137}\text{Cs}$  activity ratio was  $0.99 \pm 0.03$  adjacent to the 1F NPP during the first month of measuring data (Buessler et al., 2011), then the  $^{134}\text{Cs}/^{137}\text{Cs}$  activity ratio was assumed to be 1 on 26 March 2011. The ratio decreased with time because the half-life of  $^{134}\text{Cs}$  (2 yr) is shorter than the 30 yr half-life of  $^{137}\text{Cs}$ . Figure 3 shows the estimated rates at which  $^{131}\text{I}$ ,  $^{134}\text{Cs}$ , and  $^{137}\text{Cs}$  were directly released from the 1F NPP. The estimated total amounts of  $^{131}\text{I}$ ,  $^{134}\text{Cs}$ , and  $^{137}\text{Cs}$  directly released until the end of February 2012 were 11.1 PBq, 3.52 PBq, and 3.55 PBq, respectively. Tsumune et al. (2012) previously estimated the total amount to be 3.51 PBq by the end of May 2011. The total amount of directly released  $^{137}\text{Cs}$  activity increased by 0.04 PBq between June 2011 and February 2012. The errors associated with these estimates are at least 20%, based on the Tsumune et al. (2012) estimate that the total amount of  $^{137}\text{Cs}$  activity released by the end of May was  $3.5 \pm 0.7$  PBq. Therefore, we summarized that the estimated total amounts of  $^{131}\text{I}$ ,  $^{134}\text{Cs}$ , and  $^{137}\text{Cs}$  directly released until the end of February 2012 were  $11.1 \pm 2.2$  PBq,  $3.5 \pm 0.7$  PBq, and  $3.6 \pm 0.7$  PBq, respectively. Note that the estimated total amount of radioactivity directly released was the sum of daily releases and not corrected for radioactive decay. The radioactivity directly released by the end of May 2011 accounted for 98.8% of the total radioactivity directly released to the ocean. The rate at which  $^{137}\text{Cs}$  was directly released to the ocean (outside of port) was estimated to decrease exponentially and to be  $1.0 \times 10^{10}$  Bq day $^{-1}$  by the end of February 2012.

## 3.2 Atmospheric deposition

We used an atmospheric transport model (CAMx) to estimate wet and dry deposition rates from 11 March to 1 April 2011. Figure 4 shows cumulative atmospheric deposition from 11 March to 1 April 2011 ( $\text{Bq m}^{-2}$ ). The distribution of atmospheric deposition in the ocean was not measured on a regional scale. There were areas of high deposition of radioactivity to the northeast and southeast of the 1F NPP site in the simulation. This pattern is consistent with the global simulation of Aoyama et al. (2012c, 2013b). The total amount of radioactivity deposited from the atmosphere was 1.14 PBq within the simulated area ( $3.0 \times 10^5 \text{ km}^2$ ). A global model estimated the total amount of radioactivity deposited in this area to be 3.04 PBq (MASINGAR mk2, Yukimoto et al., 2011), a value that we used as a boundary condition in this simulation (Aoyama et al., 2012c, 2013b). Both models employed the same release rate to the atmosphere, the total release amounting to 9.0 PBq (Terada, et al., 2012). Estimations of the rates of deposition of radioactivity from the atmosphere onto the ocean are still associated with great uncertainties because the simulated results of atmospheric deposition compare poorly with observations at sea level. Aoyama et al. (2012c, 2013b) pointed out that the total amount of simulated atmospheric deposition onto the North Pacific is about 50 % of the total inventory of measurements. The estimated total amount of atmospheric deposition in this study was about one-third of the estimate derived from the global model that was used as a boundary condition.

## 3.3 Inflow from boundary sections

Aoyama et al. (2012c, 2013b) carried out 1 yr simulations of  $^{134}\text{Cs}$  and  $^{137}\text{Cs}$  activity in the North Pacific with considering atmospheric deposition and direct release. Figure 5 shows measured and simulated  $^{137}\text{Cs}$  activity in the North Pacific. Measured surface  $^{137}\text{Cs}$  activity is shown as colored circles in Fig. 5 during April–June 2011, July–September 2011, October–December 2011 and January–March 2012 (Aoyama et al., 2012c, 2013a, b). Aoyama et al. (2013a) estimated that main body of radioactive

BGD

10, 6259–6314, 2013

One-year,  
regional-scale  
simulation of  $^{137}\text{Cs}$   
radioactivity in the  
ocean

D. Tsumune et al.

Title Page

Abstract

Introduction

Conclusions

References

Tables

Figures

◀

▶

◀

▶

Back

Close

Full Screen / Esc

Printer-friendly Version

Interactive Discussion

surface plume of which activity was exceeded  $10 \text{ Bq m}^{-3}$  had been travelling along  $40^\circ \text{ N}$ , and reached International Date Line one year after the accident. Simulated surface  $^{137}\text{Cs}$  activity is shown as contour on 15 May 2011, 15 August 2011, 15 November 2011 and 15 February 2012. Simulated distributions with atmospheric deposition and direct release were in good agreement with measured one in the North Pacific. Simulated distribution with only direct release suggests that the distribution of  $^{137}\text{Cs}$  activity in April–June was mainly formed by atmospheric deposition in the whole North Pacific. We set simulated  $^{137}\text{Cs}$  activity by the North Pacific simulations to the boundary sections of a regional model off Fukushima to simulate the inflow of  $^{137}\text{Cs}$  attributable to atmospheric deposition outside the model domain.

### 3.4 Oceanic flow field

The model domain includes the mixing region between the Oyashio and Kuroshio Currents. The characteristics of the flow field are very complex because they reflect the effects of two major current systems as well as mesoscale eddies. Figure 6 shows the simulated current field on 1 May, 1 June, and 15 June 2011. The Kuroshio Current was present in the southern part of the simulated region. This simulation, which was nudged with JCOPE2 reanalysis data, depicted a mesoscale eddy adjacent to the Ibaraki coast until the end of May 2011. This mesoscale eddy was observed by satellite images of sea surface temperature and chlorophyll *a* concentrations (Fig. S3) and disappeared at the end of June. This mesoscale eddy had a dominant effect on the distribution of  $^{137}\text{Cs}$  along the Ibaraki coast (Aoyama et al., 2012b). The currents adjacent to the Ibaraki coast changed from northward to southward because of the disappearance of the mesoscale eddy at the end of May 2011.

Figure 7 shows the temporal changes of simulated current vectors adjacent to the 1F NPP. Alongshore (V-component) currents were dominant. The direction of the currents changed roughly every 3–4 days because of changes in the synoptic scale wind fields. The characteristics of the simulated results were consistent with previously observed

**BGD**

10, 6259–6314, 2013

## One-year, regional-scale simulation of $^{137}\text{Cs}$ radioactivity in the ocean

D. Tsumune et al.

Title Page

Abstract

Introduction

Conclusions

References

Tables

Figures

⏪

⏩

◀

▶

Back

Close

Full Screen / Esc

Printer-friendly Version

Interactive Discussion

results (Nakamura, 1991). Alongshore currents were associated with average current speeds of 5–6  $\text{cm s}^{-1}$  from 20 March to 20 April 2011. Temporal change of coastal currents had a dominant effect on the distribution of  $^{137}\text{Cs}$  activity in the coastal area near the 1F NPP.

### 3.5 Temporal change of $^{137}\text{Cs}$

#### 3.5.1 Sites close to the direct release point (1F NPP)

Simulated  $^{137}\text{Cs}$  activities near the 1F NPP were in good agreement with observations (Fig. 8). In the daily mean simulated and measured  $^{137}\text{Cs}$  activities (Fig. 9), there were two high-activity peaks on 26 March and 7 April 2011, during which time release rates of  $^{137}\text{Cs}$  were assumed to be constant in the simulation. The changes of  $^{137}\text{Cs}$  activity were caused by changes in the coastal current system. When the coastal current was weak on 7 April 2011 (see Fig. 7), the simulated activity was highest. This change of simulated results was consistent with measurements. TEPCO stopped the visible leakage from the intake of reactor 2 on 6 April 2011 by injecting water glass (sodium silicate) into a pit near reactor 2. The measured  $^{137}\text{Cs}$  activity was highest on 7 April 2011 because of the slow speed of the southward current just after visible leakage stopped.

Simulated  $^{137}\text{Cs}$  activities decreased exponentially after 7 April 2011. The curvature of the exponential curve changed on 26 April and 30 June 2011. There were few measured activities from July to October 2011 because of the higher detection limit of the measurements. However, high measured  $^{137}\text{Cs}$  activities coincided with high simulated activities during the period when there were few measurements. Because simulated  $^{137}\text{Cs}$  activities were underestimated after January 2012, another exponential curve should be fit to the activities after that date. However, it is difficult to parameterize a least-squares exponential curve after January 2012 because there were no measured activities less than  $1000 \text{ Bq m}^{-3}$ , the detection limit of the measurements.

BGD

10, 6259–6314, 2013

One-year,  
regional-scale  
simulation of  $^{137}\text{Cs}$   
radioactivity in the  
ocean

D. Tsumune et al.

Title Page

Abstract

Introduction

Conclusions

References

Tables

Figures

◀

▶

◀

▶

Back

Close

Full Screen / Esc

Printer-friendly Version

Interactive Discussion

Continuous measurements with a lower detection limit made adjacent to the 1F NPP would be necessary to realistically estimate direct release rates after January 2012.

Before 26 March 2011 analysis of  $^{131}\text{I}/^{137}\text{Cs}$  activity ratios has indicated that measured  $^{137}\text{Cs}$  activities were attributable to atmospheric deposition (Tsumune et al., 2012). Simulated results prior to 26 March are one or two orders of magnitude smaller than measured activities. The magnitude of atmospheric deposition into the ocean was probably underestimated because the absence of measurements of deposition on the ocean caused release rates to the atmosphere to be underestimated (Aoyama et al., 2012c, 2013b). Total deposition of  $^{137}\text{Cs}$  onto the ocean was two times smaller than measured inventories in the North Pacific outside of the area directly adjacent to the 1F NPP. These simulated results suggest that there was greater underestimation of the amount of atmospheric deposition of  $^{137}\text{Cs}$  onto the ocean in the region directly adjacent to the 1F NPP.

The differences between the ALL and D\_RELEASE scenarios of the simulated  $^{137}\text{Cs}$  activities adjacent to the 1F NPP were smaller than the simulated  $^{137}\text{Cs}$  activity in the D\_RELEASE scenario after 26 March 2011 (Fig. 10). The differences of  $^{137}\text{Cs}$  activities were attributable to atmospheric deposition. When the  $^{137}\text{Cs}$  activities attributable to atmospheric deposition were increased by about one or two orders of magnitude to correct for the underestimation of atmospheric deposition rates, the effect of atmospheric deposition on  $^{137}\text{Cs}$  activity was still negligible directly adjacent to the 1F NPP.

### 3.5.2 Sites 10 km and 16 km south from the direct release point (2F NPP and Iwasawa coast)

Figure 11 shows the measured and simulated (ALL case)  $^{137}\text{Cs}$  activities at the 2F NPP north discharge canal and offshore of Iwasawa near the 2F NPP. These discharges enter the ocean 10 km and 16 km south of the direct release point, respectively. Along-shore currents dominate physical transport in this coastal region (Fig. 7). Tsumune et al. (2012) have pointed out that the  $^{137}\text{Cs}$  activity attributable to direct release exceeded  $1.0 \times 10^6 \text{ Bq m}^{-3}$  on 27 March, decreased to  $1.0 \times 10^5 \text{ Bq m}^{-3}$  by 4 April, and

6274

**BGD**

10, 6259–6314, 2013

## One-year, regional-scale simulation of $^{137}\text{Cs}$ radioactivity in the ocean

D. Tsumune et al.

Title Page

Abstract

Introduction

Conclusions

References

Tables

Figures

◀

▶

◀

▶

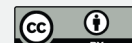
Back

Close

Full Screen / Esc

Printer-friendly Version

Interactive Discussion





then increased abruptly to more than  $1.0 \times 10^6 \text{ Bq m}^{-3}$  on 5 April. The simulation portrayed the rapid increase, which reflected an enhancement of the southward coastal current from 3 to 5 April due to a change of wind forcing (Fig. 7). Analysis of  $^{131}\text{I}/^{137}\text{Cs}$  activity ratios indicated that measured  $^{137}\text{Cs}$  activities from 27 March to the middle of April 2011 were attributable to direct releases (Tsumune et al., 2012). During this period, simulated results were in good agreement with observations.

After the middle of April 2011, simulated activities were lower than measured activities. Whereas the variations of measured  $^{137}\text{Cs}$  activities were smaller at the 2F NPP and off the Iwasawa coast than at the 1F NPP, the variations of simulated  $^{137}\text{Cs}$  activities were larger at the 2F NPP and off the Iwasawa coast than at the 1F NPP. Although the higher values of the variable simulated  $^{137}\text{Cs}$  activities were in relatively good agreement with measurements, the lower values were smaller than observations.

Analysis of  $^{131}\text{I}/^{137}\text{Cs}$  activity ratios indicated that measured  $^{137}\text{Cs}$  activities before 27 March 2011 were attributable to atmospheric deposition (Tsumune et al., 2012). Simulated activities were one or two orders of magnitude smaller than measured activities. This difference suggests that the magnitude of atmospheric deposition onto the ocean was underestimated.

The differences between simulated  $^{137}\text{Cs}$  activities estimated with the ALL and D\_RELEASE scenarios were smaller than the  $^{137}\text{Cs}$  activities simulated with the D\_RELEASE scenario after 27 March 2011 (Fig. 12). The differences of  $^{137}\text{Cs}$  activities were attributable to atmospheric deposition. Increasing the  $^{137}\text{Cs}$  activities attributable to atmospheric deposition by about one or two orders of magnitude increased the lower values of the variable simulated  $^{137}\text{Cs}$  activities. Underestimation of the simulated  $^{137}\text{Cs}$  activities at the 2F NPP and off the Iwasawa coast after the middle of April may therefore be attributable to underestimation of atmospheric deposition rates.

**BGD**

10, 6259–6314, 2013

**One-year,  
regional-scale  
simulation of  $^{137}\text{Cs}$   
radioactivity in the  
ocean**

D. Tsumune et al.

Title Page

Abstract

Introduction

Conclusions

References

Tables

Figures

◀

▶

◀

▶

Back

Close

Full Screen / Esc

Printer-friendly Version

Interactive Discussion



### 3.5.3 Offshore from the direct release point

Figure 13 shows measured  $^{137}\text{Cs}$  activities 30 km offshore. The model simulation cannot identify the differences of  $^{137}\text{Cs}$  activities at each point. Therefore, measured points are shown by the same symbol in Fig. 13, and gray shading indicates the range of simulated activities at eight sites. Here we focus on the effects of offshore transport. The averaged offshore-onshore current speed was about one-tenth the speed of the along-shore current in this region from March to May 2011 (Fig. 7). Previous model simulations nudged with HYCOM reanalysis (Tsumune et al., 2012) underestimated offshore transport because the simulated mixed layer depth was deeper than the mixed layer depth simulated by JCOPE2. Analysis of  $^{131}\text{I}/^{137}\text{Cs}$  activity ratios indicated that measured  $^{137}\text{Cs}$  activities after 9 April 2011 were attributable to direct release (Tsumune et al., 2012). Simulated  $^{137}\text{Cs}$  activities attributable to direct release were in good agreement with measurements. The model simulation nudged with JCOPE2 depicted reasonable offshore transport. One of the reasons for the improvement was the reasonable mixed layer depth in the JCOPE2 reanalysis data. Simulated  $^{137}\text{Cs}$  activities before 9 April 2011 were attributable to atmospheric deposition. The fact that simulated activities were one or two orders of magnitude smaller than measured activities before 9 April 2011 also suggests that the rates of atmospheric deposition onto the ocean were underestimated.

The differences between  $^{137}\text{Cs}$  activities simulated with the ALL and D\_RELEASE scenarios (Fig. 14) were smaller than the  $^{137}\text{Cs}$  activities simulated with the D\_RELEASE scenario after 9 April 2011. The differences of  $^{137}\text{Cs}$  activities were attributable to atmospheric deposition. Increasing the simulated  $^{137}\text{Cs}$  activity attributable to atmospheric deposition by about one or two orders of magnitude, would diminish the magnitude of the underestimation before 9 April and after 1 May.

Measurements 3–8 km and 15 km offshore started in the middle of April 2011 near the northern and southern boundaries of the 1F NPP. Although simulated  $^{137}\text{Cs}$  activities were in good agreement with measurements near the northern boundary of the

**BGD**

10, 6259–6314, 2013

**One-year,  
regional-scale  
simulation of  $^{137}\text{Cs}$   
radioactivity in the  
ocean**

D. Tsumune et al.

Title Page

Abstract

Introduction

Conclusions

References

Tables

Figures

◀

▶

◀

▶

Back

Close

Full Screen / Esc

Printer-friendly Version

Interactive Discussion

1F NPP, near the southern boundary simulated  $^{137}\text{Cs}$  activities were smaller than measured activities, especially after the end of April 2011 (Figs. S4 and S5). These patterns are consistent with the results at the 2F NPP, directly off the Iwasawa coast, and 30 km offshore.

### 3.6 Spatial distribution

The KOK cruise and observations by MEXT provided spatial distributions on a regional scale after June 2011 (Buesseler et al., 2012). Figure 15 shows simulated  $^{137}\text{Cs}$  activities in surface waters (ALL case) and at a depth of 100 m on 15 June 2011 and activities measured from 3 to 18 June 2011 by the KOK cruise. Measured and simulated  $^{137}\text{Cs}$  activities varied from  $1 \text{ Bq m}^{-3}$  to  $3000 \text{ Bq m}^{-3}$ . High  $^{137}\text{Cs}$  activities were measured off the Ibaraki coast. Simulations identified a high activity core due to transport effects by mesoscale eddies (Buesseler et al., 2012; see Fig. 5). Measured  $^{137}\text{Cs}$  activities were close to background values ( $1\text{--}2 \text{ Bq m}^{-3}$ ; HAM database; Aoyama and Hirose, 2004 and extended) in the Kuroshio region. The distributions of simulated  $^{137}\text{Cs}$  activities were in good agreement with the measured activities, even if the simulated Kuroshio path deviated a bit from the observed path.

Comparison of measured  $^{137}\text{Cs}$  activities with  $^{137}\text{Cs}$  activities simulated with the NO\_INFLOW and D\_RELEASE scenarios (Fig. 16) suggests that the high-activity core was attributable to direct release, and the activity at the eastern boundary was attributable to atmospheric deposition. The  $^{137}\text{Cs}$  activity attributable to atmospheric deposition moved beyond the domain of this model during the simulation period, and the effects of atmospheric deposition were therefore small. Fluxes from atmospheric deposition over a wider area were dominant at the northern and eastern areas of the model domain.

The KOK cruise (Buesseler et al., 2012) made it possible to investigate the vertical profile of  $^{137}\text{Cs}$  in the model domain during June 2011. Figure 17 shows measured and simulated vertical profiles (ALL scenario) of  $^{137}\text{Cs}$  activities in the area of the KOK

BGD

10, 6259–6314, 2013

## One-year, regional-scale simulation of $^{137}\text{Cs}$ radioactivity in the ocean

D. Tsumune et al.

Title Page

Abstract

Introduction

Conclusions

References

Tables

Figures

◀

▶

◀

▶

Back

Close

Full Screen / Esc

Printer-friendly Version

Interactive Discussion

---

**One-year,  
regional-scale  
simulation of  $^{137}\text{Cs}$   
radioactivity in the  
ocean**D. Tsumune et al.

---

[Title Page](#)[Abstract](#)[Introduction](#)[Conclusions](#)[References](#)[Tables](#)[Figures](#)[⏪](#)[⏩](#)[◀](#)[▶](#)[Back](#)[Close](#)[Full Screen / Esc](#)[Printer-friendly Version](#)[Interactive Discussion](#)

cruise. It is difficult to compare observations and simulations at each point because the mesoscale eddy effects cause the vertical profiles to be complex. Measured  $^{137}\text{Cs}$  activities are plotted with the same symbol, and simulated vertical profiles are plotted as continuous lines at sites where the measurements were made. Measured  $^{137}\text{Cs}$  activities varied from  $1\text{ Bq m}^{-3}$  to  $3000\text{ Bq m}^{-3}$  in the surface layer. Maximum  $^{137}\text{Cs}$  activities decreased with depth. The maximum activity was  $100\text{ Bq m}^{-3}$  and  $10\text{ Bq m}^{-3}$  at depths of 200 m and 400 m, respectively. The characteristics of simulated vertical profiles were in good agreement with observations. Measured  $^{137}\text{Cs}$  activities were higher than the background values of  $1\text{--}2\text{ Bq m}^{-3}$ .

The total  $^{137}\text{Cs}$  inventories simulated with the ALL and D\_RELEASE scenarios in the part of the model domain ( $35^{\circ} 54' \text{ N}\text{--}38^{\circ} 00' \text{ N}$ ,  $139^{\circ} 54' \text{ E}\text{--}147^{\circ} 00' \text{ E}$ ) corresponding to the area of the KOK cruise (Fig. 18) increased after 26 March 2011 because of the effect of direct release. The maximum inventory was 4 PBq in the middle of April 2011. Inventories estimated by measurements on the KOK cruise were 1.9–2.1 PBq from 3–18 June 2011. The simulated inventory was 1.7 PBq on 15 June 2011. Simulated inventories were a bit lower than measured values, perhaps because of underestimation of atmospheric deposition. Simulated results were reasonable compared to measurements. The simulated inventory attributable to direct release was 1 PBq, 60 % of the total  $^{137}\text{Cs}$  inventory.

Figure 19a and b shows the simulated  $^{137}\text{Cs}$  activities (ALL scenario) in the surface waters and at a depth of 100 m on 25 August 2011, along with the measurements made from 23–27 August 2011 by MEXT. Measured  $^{137}\text{Cs}$  activities varied from 10 to  $100\text{ Bq m}^{-3}$  in the surface water outside of the Kuroshio region. Measured  $^{137}\text{Cs}$  activities at a depth of 100 m were lower than the activities in the surface water. Simulated results depicted the characteristics of measured activities in the region even if the simulated Kuroshio path was a little different from the observed path. Figure 19c and d shows the  $^{137}\text{Cs}$  activities simulated by the D\_RELEASE scenario in surface waters and at a depth of 100 m. The effect of direct releases of  $^{137}\text{Cs}$  on activities was smaller than expected from the results of measurements made on the KOK cruise in

the middle of June 2011. The effect of direct releases on  $^{137}\text{Cs}$  activities was larger in surface waters than at a depth of 100 m.

Figure 20a and b shows the simulated  $^{137}\text{Cs}$  activities in surface waters and at a depth of 100 m on 2 December 2011 and activities measured from 30 November to 2 December 2011 by MEXT. Measured  $^{137}\text{Cs}$  activities were lower than the activities measured in August. Simulated results adequately depicted the characteristics of measurements in this region. Figure 20c and d shows the  $^{137}\text{Cs}$  activities simulated by the D\_RELEASE scenario in surface waters and at a depth of 100 m. The effect of direct releases on  $^{137}\text{Cs}$  activities was smaller compared with the results in August 2011.

## 4 Discussion

### 4.1 Contributions of atmospheric deposition, direct releases, and inflow to the regional ocean

It is important to discuss the individual contributions of atmospheric deposition, direct release, and inflow (Fig. 1) on the  $^{137}\text{Cs}$  activity in the region of the model. We used analysis of  $^{131}\text{I}/^{137}\text{Cs}$  activity ratios and the three model scenarios to identify the contributions of each of these fluxes to  $^{137}\text{Cs}$  activities (Tsumune et al., 2012). Analysis of  $^{131}\text{I}/^{137}\text{Cs}$  activity ratios indicated that the contributions of direct releases to  $^{137}\text{Cs}$  activities were dominant from 26 March to the end of May 2011 at the 1F NPP, from 27 March to the middle of April 2011 at the 2F NPP and in Iwasawa coastal waters, and from 9 April to the end of April 2011 30 km offshore (Tsumune et al., 2012). The contribution of atmospheric deposition to  $^{137}\text{Cs}$  activity was estimated to be dominant before these periods in all cases. The contributions from atmospheric deposition and inflow were distinguished by comparing the NO\_INFLOW and D\_RELEASE model simulations.

The model simulations suggested that each flux changed temporally and spatially. The contribution of atmospheric deposition to  $^{137}\text{Cs}$  activities was dominant in the

BGD

10, 6259–6314, 2013

One-year,  
regional-scale  
simulation of  $^{137}\text{Cs}$   
radioactivity in the  
ocean

D. Tsumune et al.

Title Page

Abstract

Introduction

Conclusions

References

Tables

Figures

◀

▶

◀

▶

Back

Close

Full Screen / Esc

Printer-friendly Version

Interactive Discussion

## BGD

10, 6259–6314, 2013

---

**One-year,  
regional-scale  
simulation of  $^{137}\text{Cs}$   
radioactivity in the  
ocean**

D. Tsumune et al.

---

[Title Page](#)
[Abstract](#)[Introduction](#)[Conclusions](#)[References](#)[Tables](#)[Figures](#)[⏪](#)[⏩](#)[◀](#)[▶](#)[Back](#)[Close](#)[Full Screen / Esc](#)[Printer-friendly Version](#)[Interactive Discussion](#)

model region before 26 March 2011. After 26 March the contribution of direct releases to the inventory increased (see Fig. S6 and S7). Direct releases accounted for 80 % of the total inventories in the middle of April 2011 in the region of the KOK cruise (see Fig. 18).  $^{137}\text{Cs}$  attributable to atmospheric deposition was advected out of the model domain in the middle of June 2011 (Fig. 16). The contribution of direct releases to the inventory declined because of the decrease of direct release rates. The contribution of inflow to  $^{137}\text{Cs}$  activity was dominant after the end of November 2012 (Fig. 20). Simulations identified  $^{137}\text{Cs}$  activities attributable to direct releases only along the coast by the end of February 2012 (see Fig. S8). Direct releases accounted for less than 1 % of the total inventories at the end of February 2012 (Fig. S9).

Measured  $^{137}\text{Cs}$  activities attributable to atmospheric deposition were  $1.0 \times 10^5$ – $1.0 \times 10^6$  Bq m<sup>-3</sup> adjacent to the 1F NPP before 26 March 2011,  $1.0 \times 10^4$ – $1.0 \times 10^5$  Bq m<sup>-3</sup> adjacent to the 2F NPP and in Iwasawa coastal waters after 27 March 2011, and 1000–30 000 Bq m<sup>-3</sup> 30 km offshore before 8 April 2011. Simulated activities were one or two orders of magnitudes lower than measured activities at the 1F NPP, at the 2F NPP, in Iwasawa coastal waters, and 30 km offshore. If allowance is made for the underestimation of atmospheric deposition, then underestimation of activities at the 2F NPP and in Iwasawa coastal waters might be resolved after the middle of April 2011, and underestimation 30 km offshore might be resolved after the end of April 2011. These comparisons suggest that the underestimation of atmospheric deposition onto the ocean was larger (about 2 times) in this model domain than in the North Pacific (Aoyama et al., 2013b). A realistic representation of atmospheric deposition onto the coastal zone is needed for the assessment of ocean contamination. Activities measured before the first direct releases helped to improve the accuracy of the simulated atmospheric deposition.

The fact that simulated  $^{137}\text{Cs}$  activities attributable to direct releases were in good agreement with measured activities in three time series suggests that estimates of direct release rates were reasonable. Use of JCOPE2 for nudging improved simulations of offshore transport and hence the reproducibility of  $^{137}\text{Cs}$  activities 30 km offshore

compared with a previous simulation (Tsumune et al., 2012). This result suggests that our estimated direct release rates were sufficiently accurate to simulate  $^{137}\text{Cs}$  activities in the model domain.

The fact that simulated  $^{137}\text{Cs}$  activities attributable to inflow were in good agreement with observations (Figs. 15, 16, 19, and 20) suggests that underestimation of atmospheric deposition outside of the model domain was not large. Aoyama et al. (2013b) suggested that the estimated total amount of atmospheric deposition was half the inventory in the North Pacific outside the region near the 1F NPP.

Direct release and inflow rates were adequate for the simulation of  $^{137}\text{Cs}$  activity in the model domain. Atmospheric deposition rates, however, were underestimated. Measured  $^{137}\text{Cs}$  activities attributable to atmospheric deposition helped to improve the simulated deposition rate onto the ocean.

## 4.2 Estimation of direct release rates

Other studies have not investigated the contributions of atmospheric deposition and inflow to the ocean  $^{137}\text{Cs}$  inventory. Direct release rates have been estimated by several methods and table 2 summarize estimated total amounts of  $^{137}\text{Cs}$  directly released into the ocean by the previous studies and this study.

Analysis of  $^{131}\text{I}/^{137}\text{Cs}$  activity ratios indicates that direct release of  $^{137}\text{Cs}$  activity started on 26 March 2011 (Tsumune et al., 2012). Estournel et al. (2012) pointed out that direct release may have started on 25 March 2011. We used a daily source term based on daily measurements of  $^{137}\text{Cs}$  activity to make our estimates. We used parameter studies to choose 0:00 on 26 March 2012 (JST, UTC + 9 h) as the time when direct releases of  $^{137}\text{Cs}$  activity began. It may be necessary to refine this estimate after acquiring a reasonable estimate of the effects of atmospheric deposition. The estimation of directly released  $^{137}\text{Cs}$  in this study has been based on a previous estimate (Tsumune et al., 2012) and an extended period of time. The total release was estimated to be 3.55 PBq from 26 March 2011 to the end of February 2012 with at least a 20 % error. The calculations were done in a manner similar to the estimate of  $3.5 \pm 0.7$  PBq

Title Page

Abstract

Introduction

Conclusions

References

Tables

Figures

◀

▶

◀

▶

Back

Close

Full Screen / Esc

Printer-friendly Version

Interactive Discussion

made by Tsumune et al. (2012). Directly released  $^{137}\text{Cs}$  accounted for most of the total release rate by the end of May 2011.

TEPCO estimated that the directly released  $^{137}\text{Cs}$  activity amounted to 0.94 PBq during the 5 d period from noon on 1 April 2011 to noon on 6 April 2011 (Japanese Government, 2011). TEPCO estimated the water discharge rate by using visual information on distance and the height and diameter of the flow. TEPCO then estimated the release rate of  $^{137}\text{Cs}$  activity by multiplying the flow rate ( $4.3 \text{ m}^3 \text{ h}^{-1}$ ) by the  $^{137}\text{Cs}$  activity of the contaminated water ( $1.8 \times 10^{12} \text{ Bq m}^{-3}$ ), the result being  $1.9 \times 10^{14} \text{ Bq day}^{-1}$ . They had visual information for 5 d and stopped visible leakage by injecting water glass into a pit near reactor 2 on 6 April 2011. The estimated daily release rate of  $1.9 \times 10^{14} \text{ Bq day}^{-1}$  by visual estimation is consistent with the daily release rate of  $2.2 \times 10^{14} \text{ Bq day}^{-1}$  estimated by simulation in this study and by Tsumune et al. (2012) (see Fig. 3). TEPCO also used the method of Tsumune et al. (2012) to estimate that the amount of  $^{137}\text{Cs}$  directly released from a port to the outside from 26 March to the end of September 2011 was 3.6 PBq (TEPCO, 2012b). The actual simulated value by TEPCO was 3.55 PBq by the end of September 2011, which is similar to the value estimated to the end of February 2012 in this study and by Tsumune et al. (2012). The direct release rate decreased exponentially with time and was quite small from October 2011 to February 2012.

Japan Atomic Energy Agency (JAEA) estimated the direct release rate of  $^{137}\text{Cs}$  based on TEPCO's visual estimation (Kawamura et al., 2011). They estimated that the release of  $^{137}\text{Cs}$  activity amounted to 0.94 PBq from noon on 1 April to noon on 6 April 2011 and extended that estimate before and after the period in proportion to the measured activity adjacent to the 1F NPP. Their estimate of the total release rate was 3.6 PBq from 21 March to 30 April 2011. They did not distinguish between direct release and atmospheric deposition in their estimate of the total amount of  $^{137}\text{Cs}$  activity released. JAEA validated their estimation by numerical simulation.

Institut de Radioprotection et de Sûreté Nucléaire (IRSN) in France estimated direct release rates based on measured  $^{137}\text{Cs}$  activities (Bailly du Bois et al., 2012). Their estimate of the total release was 27 PBq from 25 March to 18 July 2011. They estimated

BGD

10, 6259–6314, 2013

One-year,  
regional-scale  
simulation of  $^{137}\text{Cs}$   
radioactivity in the  
ocean

D. Tsumune et al.

Title Page

Abstract

Introduction

Conclusions

References

Tables

Figures

◀

▶

◀

▶

Back

Close

Full Screen / Esc

Printer-friendly Version

Interactive Discussion



---

**One-year,  
regional-scale  
simulation of  $^{137}\text{Cs}$   
radioactivity in the  
ocean**

D. Tsumune et al.

[Title Page](#)[Abstract](#)[Introduction](#)[Conclusions](#)[References](#)[Tables](#)[Figures](#)[⏪](#)[⏩](#)[◀](#)[▶](#)[Back](#)[Close](#)[Full Screen / Esc](#)[Printer-friendly Version](#)[Interactive Discussion](#)

the total inventory to be 11.6 PBq on 14 April 2011 from interpolation of measured data. They then extrapolated the inventory of 11.6 PBq on 14 April to 22 PBq on 8 April 2011. They extended the estimate for the period in proportion to the measured  $^{137}\text{Cs}$  activity adjacent to the 1F NPP. The estimated total amount of directly released  $^{137}\text{Cs}$  was 27 PBq from 25 March to 18 July 2011. Estournel et al. (2012) have pointed out that the inventory of 11.6 PBq on 14 April is an overestimate because of a lack of measured activities in the northern part of the 1F NPP. We also suspect that linear interpolation may not have been suitable because of the sparse data and may have caused an overestimation because the measured  $^{137}\text{Cs}$  activity decreased exponentially offshore. Estournel et al. (2012) also pointed out that temporal extrapolation is unreasonable because their own simulations indicated that the total inventory did not decrease from 8 to 14 April 2011. Our simulated results also show that the total inventory did not decrease from 8 to 14 April 2011 over a wider area (see Fig. 18). The IRSN did not validate their estimation by numerical simulation.

The Sirocco group at Toulouse University in France estimated that directly released  $^{137}\text{Cs}$  amounted to 5.1–5.5 PBq (Estournel et al., 2012). They used an inversion method based on measurements adjacent to the 1F NPP to estimate that directly released  $^{137}\text{Cs}$  amounted to 4.1–4.5 PBq. They added 1 PBq to their estimation because the simulated results were underestimated offshore compared to measured activities.

Japan Agency for Marine-Earth Science and Technology (JAMSTEC) estimated that directly released  $^{137}\text{Cs}$  amounted to 5.5–5.9 PBq by using an inversion method based on measurements not only adjacent to the 1F NPP but also at other measurement sites, mainly at the 2F NPP (Miyazawa et al., 2012b). Direct release was estimated only by using measurements made adjacent to the 1F NPP in this study because measurements at other sites were affected by transport processes and atmospheric deposition. The estimations by the Sirocco group and JAMSTEC were influenced by measurements at sites other than the site adjacent to the 1F NPP. The total amount of directly released  $^{137}\text{Cs}$  activity was estimated by numerical simulations to be  $3.5 \pm 0.7$

to 5.5–5.9 PBq. We suspect that the upper bound might be reduced if the estimated atmospheric deposition rate onto the ocean were more accurate.

Dietze and Kriest (2012) used numerical simulation to estimate that the total amount of directly released  $^{137}\text{Cs}$  was 0.94–3.5 PBq. They pointed out that their simulated results were not consistent with the IRSN estimate of 27 PBq for the total amount of  $^{137}\text{Cs}$  activity released. In contrast, Buessler et al. (2012) concluded that their data were consistent with the IRSN estimate. However, their data were collected far from the 1F NPP and in the middle of June 2011, and transport processes and atmospheric deposition affected the activities. It is therefore not suitable to use only their data to estimate the amount of directly released  $^{137}\text{Cs}$  activity. Our simulated inventory based on the total amount of released  $^{137}\text{Cs}$  activity (3.55 PBq) is consistent with their data (see Fig. 18).

In this study we assumed the discharge rate of contaminated water to be constant and that the  $^{137}\text{Cs}$  activities in the water decreased exponentially with time. The rate constant in the exponential function was determined by curve fitting. We assumed that the direct release scenario should be simple and that the exponential decrease of measured  $^{137}\text{Cs}$  activities adjacent to the 1F NPP was a reflection of direct release events. Although TEPCO visually estimated the discharge rate of contaminated water to be constant (Japanese Government, 2011), measured  $^{137}\text{Cs}$  activities adjacent to the 1F NPP varied day by day. In other studies, estimated release scenarios were variable and depended on the measured activities. Our simulated results depicted two high activity peaks adjacent to the 1F NPP from 26 March to 7 April 2011. Given the constant release scenario, the peaks were a consequence of changes in the coastal current system. Miyazawa et al. (2012b) have also pointed out that the changes of measured  $^{137}\text{Cs}$  activities were caused by changes of coastal currents. Maximum activities were measured on 7 April 2011 after visible leakage had ceased because the coastal currents were very slow at that time (see Fig. 7).

**One-year,  
regional-scale  
simulation of  $^{137}\text{Cs}$   
radioactivity in the  
ocean**

D. Tsumune et al.

Title Page

Abstract

Introduction

Conclusions

References

Tables

Figures

◀

▶

◀

▶

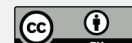
Back

Close

Full Screen / Esc

Printer-friendly Version

Interactive Discussion



### 4.3 Role of mesoscale eddy

There was a mesoscale eddy adjacent to the Ibaraki coast until the end of May (Fig. 6). Satellite images of sea surface temperature showed the mesoscale eddy adjacent to the Ibaraki coast on 14 April (Fig. S3). Satellite images of chlorophyll *a* concentrations showed offshore transport of chlorophyll *a* by the mesoscale eddy. The mesoscale eddy prevented the inflow of directly released  $^{137}\text{Cs}$  from being transported along the Ibaraki coast (Fig. S7). After 1 June the directly released  $^{137}\text{Cs}$  was advected along the Ibaraki coast (Fig. 15). The mesoscale eddy played a dominant role in the behavior of  $^{137}\text{Cs}$  off the Ibaraki coast.

Aoyama et al. (2012a, b) measured a rapid increase of  $^{137}\text{Cs}$  activity from 100 to 2000  $\text{Bq m}^{-3}$  in coastal waters off Hasaki along the southern part of the Ibaraki coast from the end of May to the first of June 2011. Measured  $^{137}\text{Cs}$  activities were low because of the mesoscale eddy off the Ibaraki coast until the end of May 2011, whereas after the disappearance of the mesoscale eddy  $^{137}\text{Cs}$  was advected southward along the Ibaraki coast. The  $^{137}\text{Cs}$  activity therefore increased rapidly at Hasaki. This model depicts the increase of  $^{137}\text{Cs}$  activity along the Ibaraki coast by the first of June 2011 (Fig. 15). However, a model without freshwater influxes from rivers cannot quantitatively represent the rapid increase of  $^{137}\text{Cs}$  activity at Hasaki because such a model fails to correctly represent coastal currents. Freshwater influxes from the many small rivers along the Fukushima and Ibaraki coasts enhance the southward current along the coast. The effect of these rivers should be considered in future refinements of the model to improve the accuracy of the simulation.

## 5 Conclusions

We carried out a 1 yr, regional-scale simulation of  $^{137}\text{Cs}$  activities in the ocean off Fukushima Japan, the sources of  $^{137}\text{Cs}$  activity being direct release, atmospheric deposition, and inflow of  $^{137}\text{Cs}$  deposited on the ocean outside the domain of the model.

BGD

10, 6259–6314, 2013

One-year,  
regional-scale  
simulation of  $^{137}\text{Cs}$   
radioactivity in the  
ocean

D. Tsumune et al.

Title Page

Abstract

Introduction

Conclusions

References

Tables

Figures

◀

▶

◀

▶

Back

Close

Full Screen / Esc

Printer-friendly Version

Interactive Discussion

## One-year, regional-scale simulation of $^{137}\text{Cs}$ radioactivity in the ocean

D. Tsumune et al.

[Title Page](#)

[Abstract](#)

[Introduction](#)

[Conclusions](#)

[References](#)

[Tables](#)

[Figures](#)

[⏪](#)

[⏩](#)

[◀](#)

[▶](#)

[Back](#)

[Close](#)

[Full Screen / Esc](#)

[Printer-friendly Version](#)

[Interactive Discussion](#)

The rates of direct release of  $^{131}\text{I}$ ,  $^{134}\text{Cs}$ , and  $^{137}\text{Cs}$  were estimated for 1 yr after the 1F NPP accident by comparing simulated results and measured activities. The estimated total amount of directly released  $^{131}\text{I}$ ,  $^{134}\text{Cs}$ , and  $^{137}\text{Cs}$  by the end of February 2012 were  $11.1 \pm 2.2$  PBq,  $3.5 \pm 0.7$  PBq, and  $3.6 \pm 0.7$  PBq, respectively. The total amount of directly released  $^{137}\text{Cs}$  activity increased by 0.04 PBq between June 2011 and February 2012. We used an atmospheric transport model with atmospheric release rates to estimate atmospheric deposition onto the ocean.

We analyzed  $^{131}\text{I}/^{137}\text{Cs}$  activity ratios to investigate the contributions of each source of  $^{137}\text{Cs}$  (Tsumune et al., 2012) and compared simulated results and measured activities. The fact that simulated  $^{137}\text{Cs}$  activities attributable to direct release were in good agreement with measurements suggests that the estimated direct release rates were reasonable. Employment of JCOPE2 instead of HYCOM for nudging improved both the offshore transport result and the reproducibility of  $^{137}\text{Cs}$  activities 30 km offshore. Simulated  $^{137}\text{Cs}$  activities attributable to atmospheric deposition were underestimated relative to observations. The rate of atmospheric deposition onto the ocean was underestimated compared to measurements because of a lack of measurements of deposition itself when atmospheric deposition rates were estimated. Measured  $^{137}\text{Cs}$  activities attributable to atmospheric deposition helped to improve the ability of simulated atmospheric deposition rates to reproduce observations. Simulated  $^{137}\text{Cs}$  activities attributable to inflow of  $^{137}\text{Cs}$  deposited onto the ocean outside the domain of the model were in good agreement with measurements in the open ocean in the model domain after June 2012.

Although the contribution of inflow increased with time and was dominant by the end of February 2012, the activity associated with directly released  $^{137}\text{Cs}$  decreased exponentially with time and was present only in the coastal zone by the end of February 2012.

Supplementary material related to this article is available online at:  
[http://www.biogeosciences-discuss.net/10/6259/2013/  
bgd-10-6259-2013-supplement.pdf](http://www.biogeosciences-discuss.net/10/6259/2013/bgd-10-6259-2013-supplement.pdf).

*Acknowledgements.* We thank members of the Earthquake Disaster Response Working Group of the Oceanographic Society of Japan led by Motoyoshi Ikeda for their helpful discussion. We also thank Yukio Masumoto, Yoshimasa Miyazawa, and Ruochao Zhang for providing the JCOPE2 results; Hiromaru Hirakuchi and Atsushi Hashimoto for providing the NuWFAS results; Taichu Y. Tanaka, Mizuo Kajiono and Tsuyoshi Thomas Sekiyama for providing the atmospheric deposition data in the North Pacific; and Mitsuhiro Toratani for providing the satellite image. We thank Fukiko Taguchi and Ryosuke Niwa for their technical support with the numerical simulation and preparation of figures. This work was supported by JSPS KAKENHI Grant Number 24110006.

## References

- Aoyama, M. and Hirose, K.: Artificial radionuclides database in the Pacific Ocean: ham database, *Scientific World Journal*, 4, 200–215, 2004.
- Aoyama, M., Tsumune, D., and Hamajima, Y.: Distribution of  $^{137}\text{Cs}$  and  $^{134}\text{Cs}$  in the North Pacific Ocean: impacts of the TEPCO Fukushima-Daiichi NPP accident, *J. Radioanal. Nucl. Ch.*, 296, 535–539, doi:10.1007/s10967-012-2033-2, 2012a.
- Aoyama, M., Tsumune, D., Uematsu, M., Kondo, F., and Hamajima, Y.: Temporal variation of  $^{134}\text{Cs}$  and  $^{137}\text{Cs}$  activities in surface water at stations along the coastline near the Fukushima Dai-ichi nuclear power plant accident site, Japan, *Geochem. J.*, 46, 321–325, 2012b.
- Aoyama, M., Kajino, M., Tanaka, T. Y., Sekiyama, T. T., Tsumune, D., Tsubono, T., Hamajima, Y., Gamo, T., Uematsu, M., Kawano, Murata, A., Kumamoto, Y., Fukasawa, M., and Chino, M.: North Pacific distribution and budget of radiocesium released by the 2011 Fukushima nuclear accident, available at: <http://nsed.jaea.go.jp/ers/environment/envs/FukushimaWS/souhoushutsu.pdf>, 2012c (in Japanese).

BGD

10, 6259–6314, 2013

## One-year, regional-scale simulation of $^{137}\text{Cs}$ radioactivity in the ocean

D. Tsumune et al.

Title Page

Abstract

Introduction

Conclusions

References

Tables

Figures

◀

▶

◀

▶

Back

Close

Full Screen / Esc

Printer-friendly Version

Interactive Discussion

---

**One-year,  
regional-scale  
simulation of <sup>137</sup>Cs  
radioactivity in the  
ocean**

D. Tsumune et al.

---

Title Page

Abstract

Introduction

Conclusions

References

Tables

Figures

◀

▶

◀

▶

Back

Close

Full Screen / Esc

Printer-friendly Version

Interactive Discussion

Aoyama, M., Uematsu, M., Tsumune, D., and Hamajima, Y.: Surface pathway of radioactive plume of TEPCO Fukushima NPP1 released <sup>134</sup>Cs and <sup>137</sup>Cs, *Biogeosciences Discuss.*, 10, 265–283, doi:10.5194/bgd-10-265-2013, 2013a.

Aoyama, M., Kajino, M., Tanaka, T. Y., Sekiyama, T. T., Tsumune, D., Tsubono, T., Hamajima, Y., Gamou, T., Uematsu, M., Kawano, T., Murata, A., Kumamoto, Y., Fukasawa, M., and Chino, M.: Spatial and temporal variations and budget of radiocesium in the North Pacific Ocean released from the 2011 Fukushima nuclear accident, in preparation, 2013b.

Bailly du Bois, P., Laguionie, P., Boust, D., Korsakissok, I., Didier, D., and Fiévet, B.: Estimation of marine source-term following Fukushima Dai-ichi accident, *J. Environ. Radioact.*, 114, 2–9, doi:10.1016/j.jenvrad.2011.11.015, 2012.

Buesseler, K., Aoyama, M., and Fukasawa, M.: Impacts of the Fukushima nuclear power plants on marine radioactivity, *Environ. Sci. Technol.*, 45, 9931–9935, doi:10.1021/es202816c, 2011.

Buesseler, K. O., Jayne, S. R., Fisher, N. S., Rypina, I. I., Baumann, H., Baumann, Z., Breier, C. F., Douglass, E. M., George, J., and Macdonald, A. M.: Fukushima-derived radionuclides in the ocean and biota off Japan, *Proc. Natl. Acad. Sci. USA*, 109, 5984–5988, 2012.

Chassignet, E. P., Hurlburt, H. E., Smedstad, O. M., Halliwell, G. R., Wallcraft, A. J., Metzger, E. J., Blanton, B. O., Lozano, C., Rao, D. B., Hogan, P. J., Srinivasan, A.: Generalized vertical coordinates for eddy—resolving global and coastal ocean forecasts, *Oceanography*, 19, 20–31, 2006.

Dietze, H. and Kriest, I.: <sup>137</sup>Cs off Fukushima Dai-ichi, Japan – model based estimates of dilution and fate, *Ocean Sci.*, 8, 319–332, doi:10.5194/os-8-319-2012, 2012.

ENVIRON International Corporation: CAMx USER'S GUIDE, 280 pp., 2009.

Estournel, C., Bosc, E., Bocquet, M., Ulses, C., Marsaleix, P., Winiarek, V., Osvath, I., Nguyen, C., Duhaut, T., Lyard, F., Michaud, H., and Auclair, F.: Assessment of the amount of Cesium-137 released into the Pacific Ocean after the Fukushima accident and analysis of its dispersion in Japanese coastal waters, *J. Geophys. Res.*, 117, C11014, doi:10.1029/2012JC007933, 2012.

Hashimoto, A., Hirakuchi, H., Toyoda, Y., and Nakaya, K.: Prediction of regional climate change over Japan due to global warming (Part 1) – evaluation of Numerical Weather Forecasting and Analysis System (NuWFAS) applied to a long-term climate simulation (in Japanese), CRIEPI report, N10044, 2010.

## One-year, regional-scale simulation of $^{137}\text{Cs}$ radioactivity in the ocean

D. Tsumune et al.

Title Page

Abstract

Introduction

Conclusions

References

Tables

Figures

◀

▶

◀

▶

Back

Close

Full Screen / Esc

Printer-friendly Version

Interactive Discussion

Honda, M. C., Aono, T., Aoyama, M., Hamajima, Y., Kawakami, H., Kitamura, M., Masumoto, Y., Miyazawa, Y., Takigawa, M., and Saino, T.: Dispersion of artificial caesium-134 and-137 in the western North Pacific one month after the Fukushima accident, *Geochem. J.*, 46, e1–e9, 2012.

5 Japanese Government: Report of Japanese Government to the IAEA Ministerial Conference on Nuclear Safety – The Accident at TEPCO’s Fukushima Nuclear Power Stations, available at: [http://www.kantei.go.jp/foreign/kan/topics/201106/iaea\\_houkokusho\\_e.html](http://www.kantei.go.jp/foreign/kan/topics/201106/iaea_houkokusho_e.html), 2011, last access: 20 December 2012.

10 Kawamura, H., Kobayashi, T., Furuno, A., In, T., Iishikawa, Y., Nakayama, T., Shima, S., and Awaji, T.: Preliminary numerical experiments on oceanic dispersion of  $^{131}\text{I}$  and  $^{137}\text{Cs}$  discharged into the ocean because of the Fukushima Daiichi nuclear power plant disaster, *J. Nucl. Sci. Tech.*, 48, 1349–1356, 2011.

15 Kinoshita, N. Sueki, K., Sasa, K., Kitagawa, J., Ikarashi, S., Nishimura, T., Wong, Y. S., Satou, Y., Handa, K., Takahashi, T., Sato, M., and Yamagata, T.: Assessment of individual radionuclide distributions from the Fukushima nuclear accident covering central-east Japan, *Proc. Natl. Acad. Sci. USA*, 108, 19526–19529, 2011.

Large, W. G. and Yeager, S. G.: Diurnal to decadal global forcing for ocean and sea-ice models: the data sets and flux climatologies, NCAR Technical Note NCAR/TN–460+STR, 111 pp., 2004.

20 Large, W. G., McWilliams, J. C., and Doney, S. C.: Ocean vertical mixing: a review and a model with a nonlocal boundary layer parameterization, *Rev. Geophys.*, 32, 363–403, 1994.

Masumoto, Y., Miyazawa, Y., Tsumune, D., Tsubono, T., Kobayashi, T., Kawamura, H., Estournel, C., Marsaleix, P., Lanerolle, L., Mehra, A., and Garraffo, Z. D.: Oceanic dispersion simulations of  $^{137}\text{Cs}$  released from the Fukushima Daiichi nuclear power plant, *Elements*, 8, 207–212, doi:10.2113/gselements.8.3.207, 2012.

25 MEXT, available at: <http://radioactivity.mext.go.jp/en/list/205/list-1.html>, last access: 20 December 2012.

Miyazawa, Y., Zhang, R., Guo, X., Tamura, H., Ambe, D., Lee, J- S., Okuno, A., Yoshinari, H., Setou, T., and Komatsu, K.: Water mass variability in the western North Pacific detected in a 15-year eddy resolving ocean reanalysis, *J. Oceanogr.*, 65, 737–756, 2009.

30 Miyazawa, Y., Masumoto, Y., Sergey M. Varlamov, S. M., and Miyama, T.: Transport simulation of the radionuclide from the shelf to open ocean around Fukushima, *Cont. Shelf Res.*, 50–51, 16–29, 2012a.

One-year,  
regional-scale  
simulation of  $^{137}\text{Cs}$   
radioactivity in the  
ocean

D. Tsumune et al.

Title Page

Abstract

Introduction

Conclusions

References

Tables

Figures

◀

▶

◀

▶

Back

Close

Full Screen / Esc

Printer-friendly Version

Interactive Discussion

- Miyazawa, Y., Masumoto, Y., Varlamov, S. M., Miyama, T., Takigawa, M., Honda, M., and Saino, T.: Inverse estimation of source parameters of oceanic radioactivity dispersion models associated with the Fukushima accident, *Biogeosciences Discuss.*, 9, 13783–13816, doi:10.5194/bgd-9-13783-2012, 2012b.
- 5 Nakamura, Y.: Studies on the Fishing Ground Formation of Sakhalin Surf Clam and the Hydraulic Environment in Coastal Region, Fukushima suisan shikenjo research report, available at: <http://www.pref.fukushima.jp/suisan-shiken/houkoku/kenpou/index.htm>, 1991 (in Japanese).
- Shchepetkin, A. F. and McWilliams, J. C.: The Regional Ocean Modeling System (ROMS): a split-explicit, free-surface, topography following coordinates oceanic model, *Ocean Model.*, 10 9, 347–404, 2005.
- Skamarock, W. C., Klemp, J. B., Dudhia, J., Gill, D. O., Barker, D. M., Duda, M., Huang, H., Wang, W., and Powers, J. G.: A description of the advanced research WRF version 3, NCAR Tech. Note NCAR/TN-475+STR, 113pp., 2008.
- 15 Tateda, Y., Tsumune, D., and Tsubono, T.: Simulation of radioactive Cs transfer in the southern Fukushima coastal biota by dynamic food chain transfer model, *J. Environ. Radioact.*, in press, doi:10.1016/j.jenvrad.2013.03.007, 2013.
- TEPCO: available at: <http://www.tepco.co.jp/en/nu/fukushima-np/f1/smp/index-e.html>, (last access: 20 December 2012), 2012a.
- 20 TEPCO: Fukushima Nuclear Accidents Investigation Report, <http://www.tepco.co.jp/en/nu/fukushima-np/interim/index-e.html>, (last access: 20 December 2012), 2012b.
- Terada, H., Katata, G., Chino, M., and Nagai, H.: Atmospheric discharge and dispersion of radionuclides during the Fukushima Dai-ichi Nuclear Power Plant accident, Part II: Verification of the source term and analysis of regional-scale atmospheric dispersion, *J. Environ. Radioact.*, 112, 141–154, 2012.
- 25 Tsumune, D., Aoyama, M., Hirose, K., Bryan, F. O., Lindsay, K., and Danabasoglu, G.: Transport of  $^{137}\text{Cs}$  to the Southern Hemisphere in an ocean general circulation model, *Prog. Oceanogr.*, 89, 38–48, doi:10.1016/j.pcean.2010.12.006, 2011.
- Tsumune, D., Tsubono, T., Aoyama, M., and Hirose, K.: Distribution of oceanic  $^{137}\text{Cs}$  from the Fukushima Dai-ichi nuclear power plant simulated numerically by a regional ocean model, *J. Environ. Radioact.*, 111, 100–108, doi:10.1016/j.jenvrad.2011.10.007, 2012.
- 30 Yukimoto, S., Yoshimura, H., Hosaka, M., Sakami, T., Tsujino, H., Hirabara, M., Tanaka, T. Y., Deushi, M., Obata, A., Nakano, H., Adachi, Y., Shindo, E., Yabu, S., Ose, T., and Kitoh, A.:



**BGD**

10, 6259–6314, 2013

**One-year,  
regional-scale  
simulation of  $^{137}\text{Cs}$   
radioactivity in the  
ocean**

D. Tsumune et al.

Title Page

Abstract

Introduction

Conclusions

References

Tables

Figures



Back

Close

Full Screen / Esc

Printer-friendly Version

Interactive Discussion

**BGD**

10, 6259–6314, 2013

**One-year,  
regional-scale  
simulation of <sup>137</sup>Cs  
radioactivity in the  
ocean**

D. Tsumune et al.

[Title Page](#)[Abstract](#)[Introduction](#)[Conclusions](#)[References](#)[Tables](#)[Figures](#)[◀](#)[▶](#)[◀](#)[▶](#)[Back](#)[Close](#)[Full Screen / Esc](#)[Printer-friendly Version](#)[Interactive Discussion](#)**Table 1.** Simulation scenarios.

Scenario name	Input sources
ALL	Direct release + Atmospheric deposition + Inflow
NO_INFLOW	Direct release + Atmospheric deposition
D_RELEASE	Direct release

## One-year, regional-scale simulation of $^{137}\text{Cs}$ radioactivity in the ocean

D. Tsumune et al.

[Title Page](#)
[Abstract](#)
[Introduction](#)
[Conclusions](#)
[References](#)
[Tables](#)
[Figures](#)
[◀](#)
[▶](#)
[◀](#)
[▶](#)
[Back](#)
[Close](#)
[Full Screen / Esc](#)
[Printer-friendly Version](#)
[Interactive Discussion](#)

**Table 2.** Estimated total amount of  $^{137}\text{Cs}$  activity (PBq) directly released into the ocean.

Organization	Period	Total amount of directly released $^{137}\text{Cs}$ (PBq = $10^{15}$ Bq)	Method	Reference
CRIEPI	26 Mar 2011 to 31 May 2011	$3.5 \pm 0.7$	Inverse method based on averaged measured activity from 26 Mar to 6 Apr	Tsumune et al. (2012)
CRIEPI	26 Mar 2011 to 29 Feb 2012	$3.6 \pm 0.7$ ( $11.1 \pm 2.2$ for $^{131}\text{I}$ , $3.5 \pm 0.7$ for $^{134}\text{Cs}$ )	Based on the method by Tsumune et al. (2012) and expanded	This study
TEPCO	Noon 1 April 2011 to Noon 6 April 2011	0.94	Flow rate estimated by visual observation $\times$ measured activity	Japanese Government (2011)
TEPCO	26 Mar 2011 to 30 Sep 2011	3.6 (11 for $^{131}\text{I}$ , 3.5 for $^{134}\text{Cs}$ )	Based on the method by Tsumune et al. (2012) and expanded	TEPCO (2012)
JAEA	21 Mar 2011 to 30 April 2011	3.6 (11 for $^{131}\text{I}$ )	Based on the estimation by TEPCO (1–6 Apr) and the expansion period (21 Mar to 30 Apr) in proportion to measured activity	Kawamura et al. (2011)
JAMSTEC	21 Mar 2011 to 30 April 2011	5.5–5.9	Inversion method based on measured activity	Miyazawa et al. (2012)
IRSN	25 Mar 2011 to 18 Jul 2011	27 (12–41)	Estimation of inventory in the ocean by observations and the expansion period (25 Mar to 18 Jul) in proportion to measured activity	Bailly du Bois et al. (2012)
Sirocco	20 Mar 2011 to 30 June 2011	5.1–5.5	Inversion method based on measured activity	Estournel et al. (2012)

## One-year, regional-scale simulation of $^{137}\text{Cs}$ radioactivity in the ocean

D. Tsumune et al.

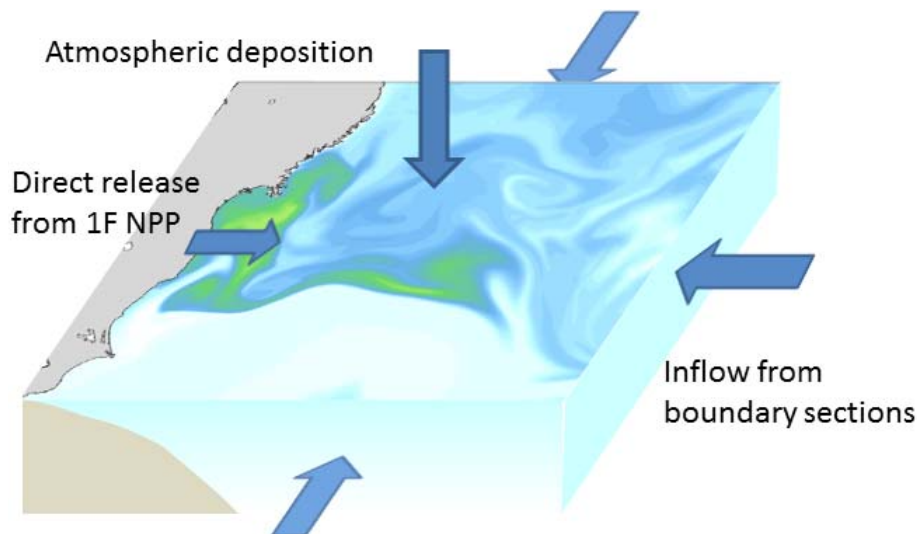


**Fig. 1.** Schematic representation of inputs of radionuclides into the model domain. Mechanisms include direct release from the 1F NPP, atmospheric deposition, and inflow of radionuclides deposited on the ocean outside the model domain.

[Title Page](#)

[Abstract](#)

[Introduction](#)

[Conclusions](#)

[References](#)

[Tables](#)

[Figures](#)

[◀](#)

[▶](#)

[◀](#)

[▶](#)

[Back](#)

[Close](#)

[Full Screen / Esc](#)

[Printer-friendly Version](#)

[Interactive Discussion](#)

## One-year, regional-scale simulation of $^{137}\text{Cs}$ radioactivity in the ocean

D. Tsumune et al.

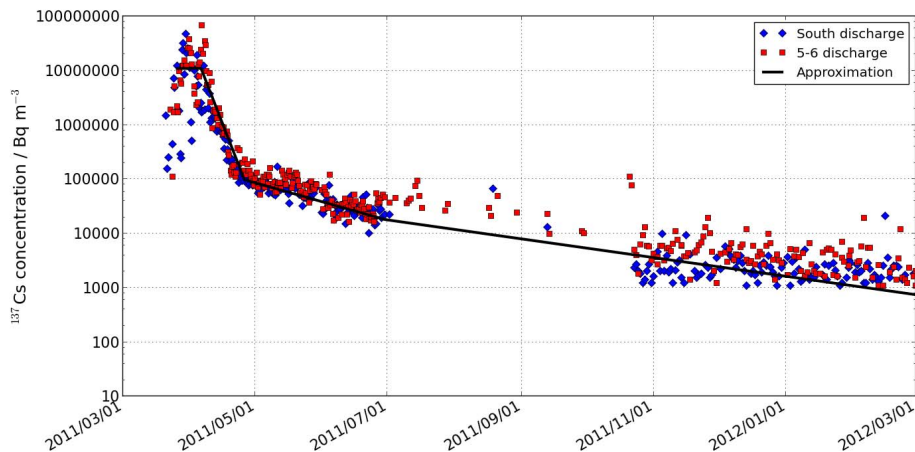


**Fig. 2.**  $^{137}\text{Cs}$  activity ( $\text{Bq m}^{-3}$ ) at the 5–6 and south discharge canals near the 1F NPP site. Gray line is the exponential curve fit to the  $^{137}\text{Cs}$  activity at both canals.

[Title Page](#)[Abstract](#)[Introduction](#)[Conclusions](#)[References](#)[Tables](#)[Figures](#)[◀](#)[▶](#)[◀](#)[▶](#)[Back](#)[Close](#)[Full Screen / Esc](#)[Printer-friendly Version](#)[Interactive Discussion](#)

## One-year, regional-scale simulation of $^{137}\text{Cs}$ radioactivity in the ocean

D. Tsumune et al.

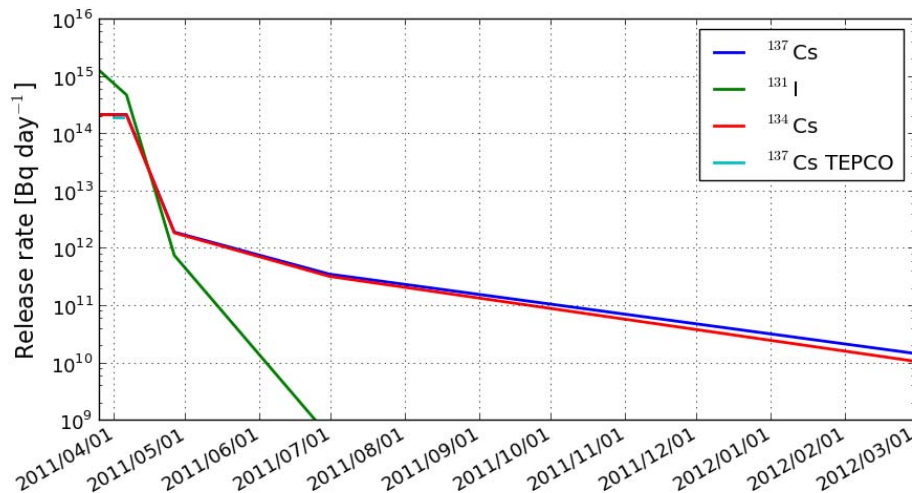


Fig. 3. Estimated direct release rates ( $\text{Bq day}^{-1}$ ) of  $^{131}\text{I}$ ,  $^{134}\text{Cs}$ , and  $^{137}\text{Cs}$  from the 1F NPP.

[Title Page](#)[Abstract](#)[Introduction](#)[Conclusions](#)[References](#)[Tables](#)[Figures](#)[⏪](#)[⏩](#)[◀](#)[▶](#)[Back](#)[Close](#)[Full Screen / Esc](#)[Printer-friendly Version](#)[Interactive Discussion](#)

**One-year, regional-scale simulation of <sup>137</sup>Cs radioactivity in the ocean**

D. Tsumune et al.

[Title Page](#)

[Abstract](#)

[Introduction](#)

[Conclusions](#)

[References](#)

[Tables](#)

[Figures](#)

◀

▶

◀

▶

[Back](#)

[Close](#)

[Full Screen / Esc](#)

[Printer-friendly Version](#)

[Interactive Discussion](#)

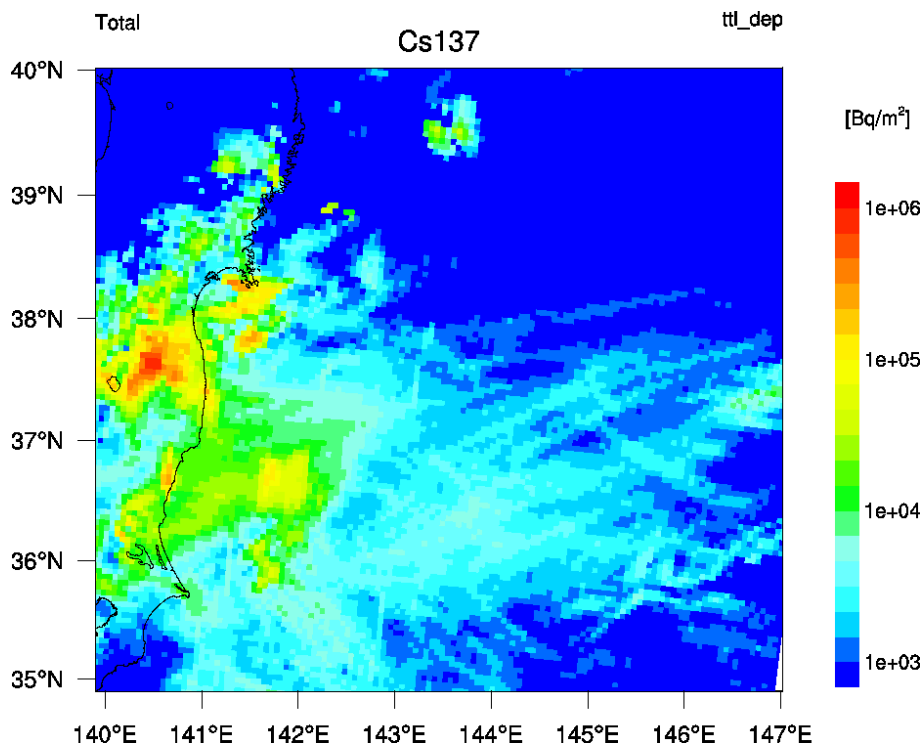


**Fig. 4.** Cumulative atmospheric deposition ( $\text{Bq m}^{-2}$ ) from 11 March to 1 April 2011.

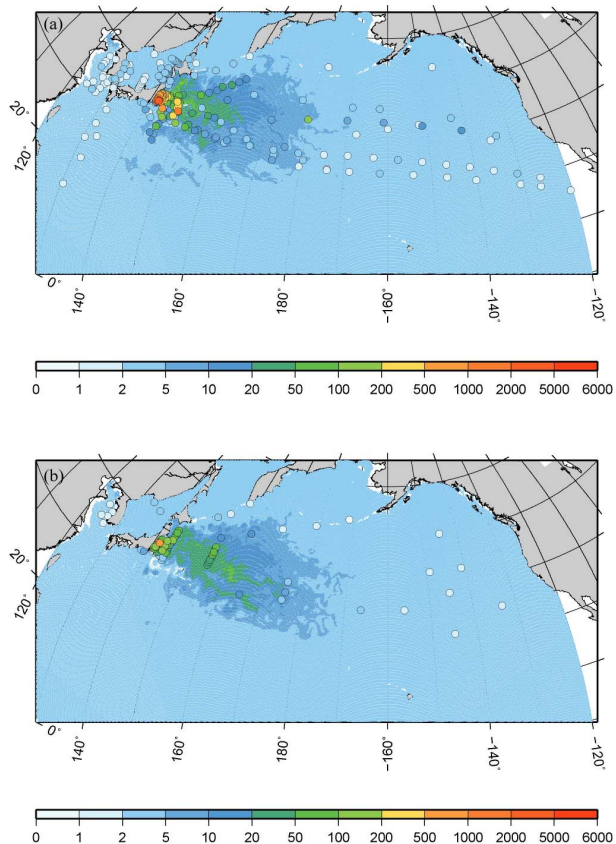


**Fig. 5a.** Simulated  $^{137}\text{Cs}$  activities ( $\text{Bq m}^{-3}$ ) in surface waters **(a)** on 15 May 2011 and measurements from April to June 2011; **(b)** on 15 August 2011 and measurements from July to September 2011 (Aoyama et al., 2012c, 2013b).

One-year, regional-scale simulation of  $^{137}\text{Cs}$  radioactivity in the ocean

D. Tsumune et al.

Title Page

Abstract

Introduction

Conclusions

References

Tables

Figures

◀

▶

◀

▶

Back

Close

Full Screen / Esc

Printer-friendly Version

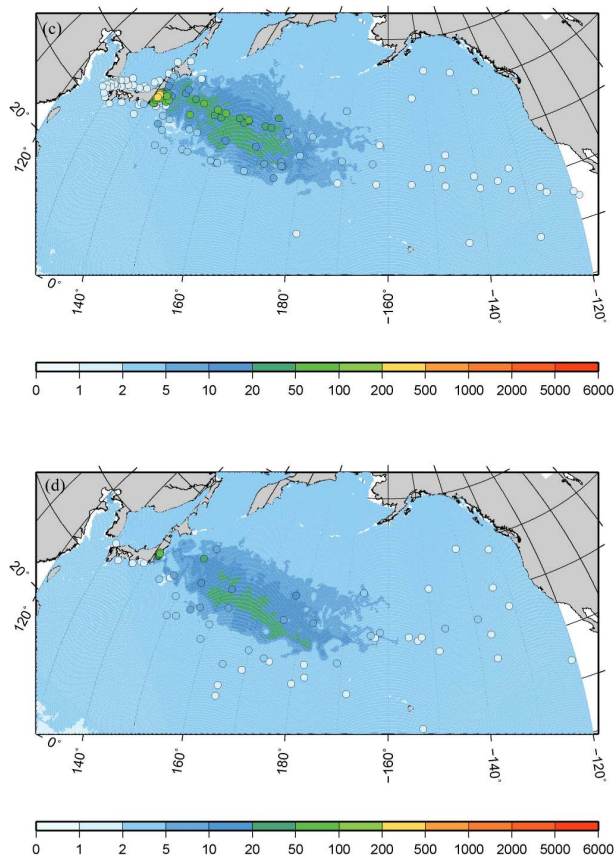
Interactive Discussion





## One-year, regional-scale simulation of $^{137}\text{Cs}$ radioactivity in the ocean

D. Tsumune et al.

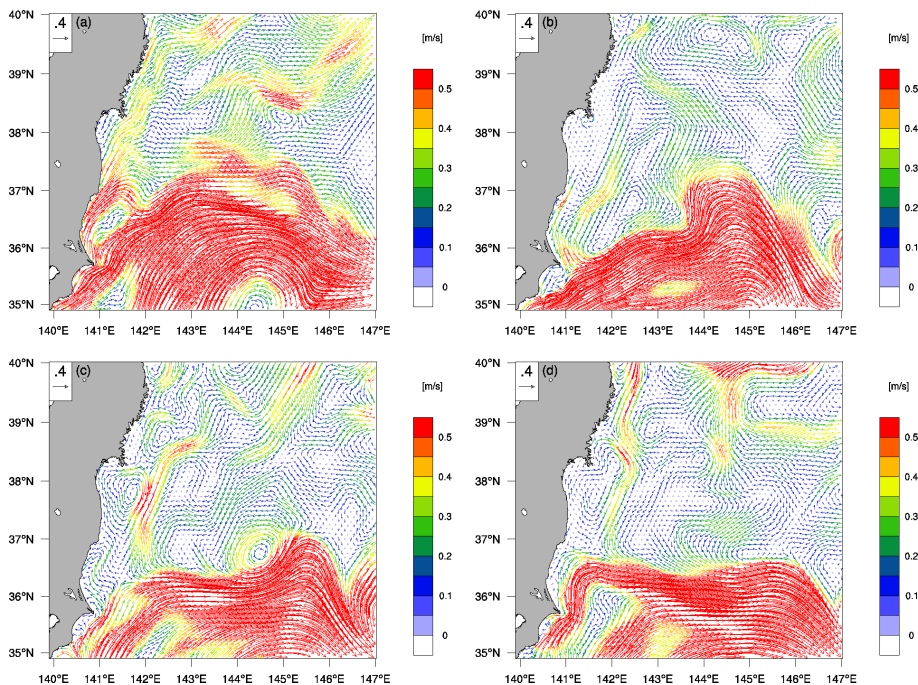


**Fig. 5b.** Simulated  $^{137}\text{Cs}$  activities ( $\text{Bq m}^{-3}$ ) in surface waters **(c)** on 15 November 2011 and measurements from October to December 2011; **(d)** on 15 February 2011 and measurements from January to March 2012 (Aoyama et al., 2012c, 2013b).

[Title Page](#)[Abstract](#)[Introduction](#)[Conclusions](#)[References](#)[Tables](#)[Figures](#)[◀](#)[▶](#)[◀](#)[▶](#)[Back](#)[Close](#)[Full Screen / Esc](#)[Printer-friendly Version](#)[Interactive Discussion](#)

# One-year, regional-scale simulation of $^{137}\text{Cs}$ radioactivity in the ocean

D. Tsumune et al.

[Title Page](#)[Abstract](#)[Introduction](#)[Conclusions](#)[References](#)[Tables](#)[Figures](#)[⏪](#)[⏩](#)[◀](#)[▶](#)[Back](#)[Close](#)[Full Screen / Esc](#)[Printer-friendly Version](#)[Interactive Discussion](#)

**Fig. 6.** Simulated current field ( $\text{ms}^{-1}$ ) on (a) 1 May, (b) 1 June, (c) 15 June, and (d) 1 July 2011.

## One-year, regional-scale simulation of $^{137}\text{Cs}$ radioactivity in the ocean

D. Tsumune et al.

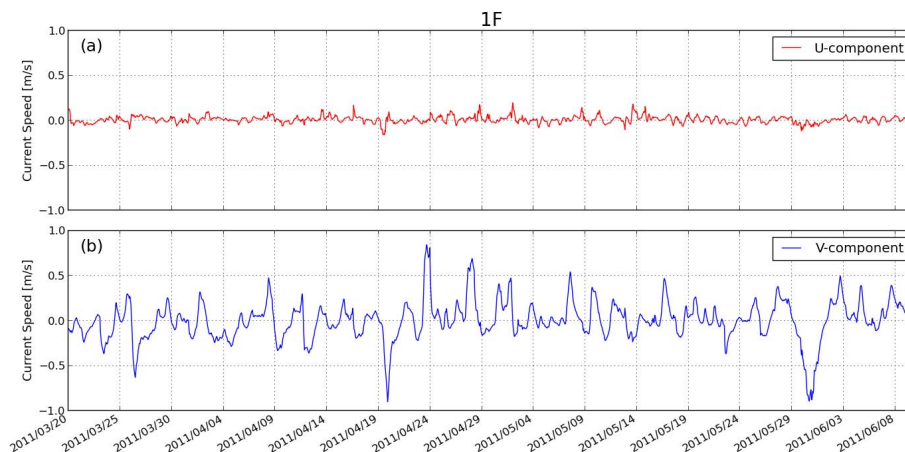


**Fig. 7.** Simulated current vectors ( $\text{ms}^{-1}$ ) adjacent to the 1F NPP. **(a)** The U-component is the net east-west speed toward the east. **(b)** The V-component is the net north-south speed toward the north.

[Title Page](#)[Abstract](#)[Introduction](#)[Conclusions](#)[References](#)[Tables](#)[Figures](#)[◀](#)[▶](#)[◀](#)[▶](#)[Back](#)[Close](#)[Full Screen / Esc](#)[Printer-friendly Version](#)[Interactive Discussion](#)

## One-year, regional-scale simulation of $^{137}\text{Cs}$ radioactivity in the ocean

D. Tsumune et al.

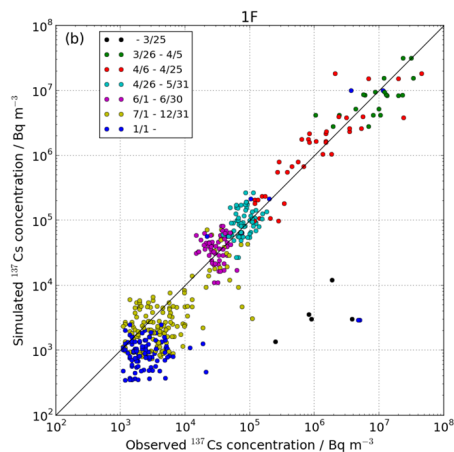
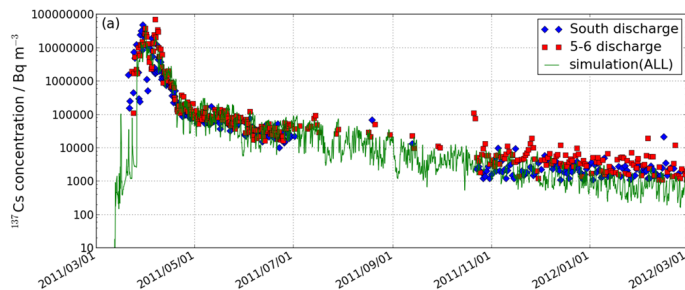


**Fig. 8.** (a) Measured  $^{137}\text{Cs}$  activities ( $\text{Bq m}^{-3}$ ) at the 5–6 (north) and south discharge canals near the 1F NPP and simulated  $^{137}\text{Cs}$  activities in a grid adjacent to the 1F NPP site (ALL scenario). (b) Scatter plot between daily mean measured activities and simulated activities.

[Title Page](#)
[Abstract](#)
[Introduction](#)
[Conclusions](#)
[References](#)
[Tables](#)
[Figures](#)
[◀](#)
[▶](#)
[◀](#)
[▶](#)
[Back](#)
[Close](#)
[Full Screen / Esc](#)
[Printer-friendly Version](#)
[Interactive Discussion](#)

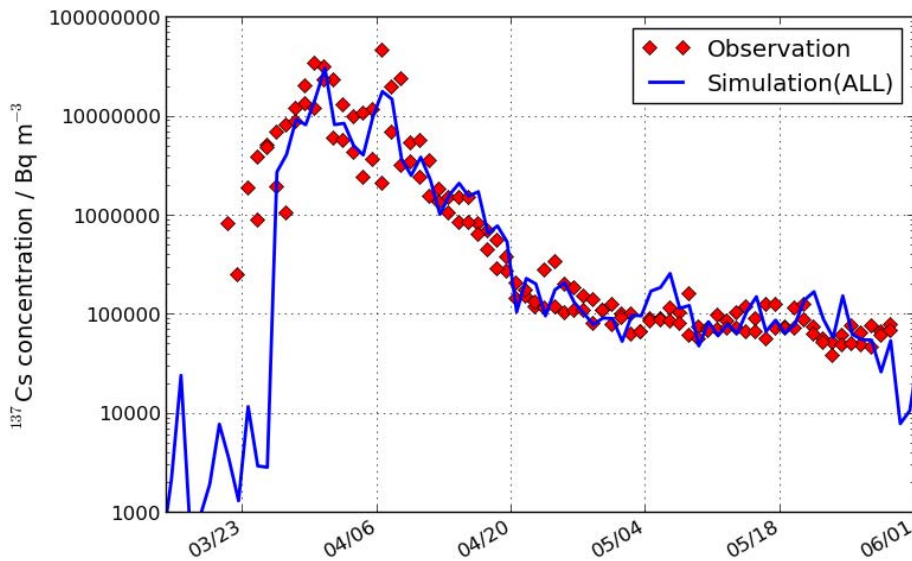


**Fig. 9.** Daily mean measured  $^{137}\text{Cs}$  activities ( $\text{Bq m}^{-3}$ ) at the 5–6 and south discharge canals and simulated activities (ALL scenario) adjacent to the 1F NPP.

**One-year, regional-scale simulation of  $^{137}\text{Cs}$  radioactivity in the ocean**

D. Tsumune et al.

[Title Page](#)

[Abstract](#)   [Introduction](#)

[Conclusions](#)   [References](#)

[Tables](#)   [Figures](#)

[◀](#)   [▶](#)

[◀](#)   [▶](#)

[Back](#)   [Close](#)

[Full Screen / Esc](#)

[Printer-friendly Version](#)

[Interactive Discussion](#)



## One-year, regional-scale simulation of $^{137}\text{Cs}$ radioactivity in the ocean

D. Tsumune et al.

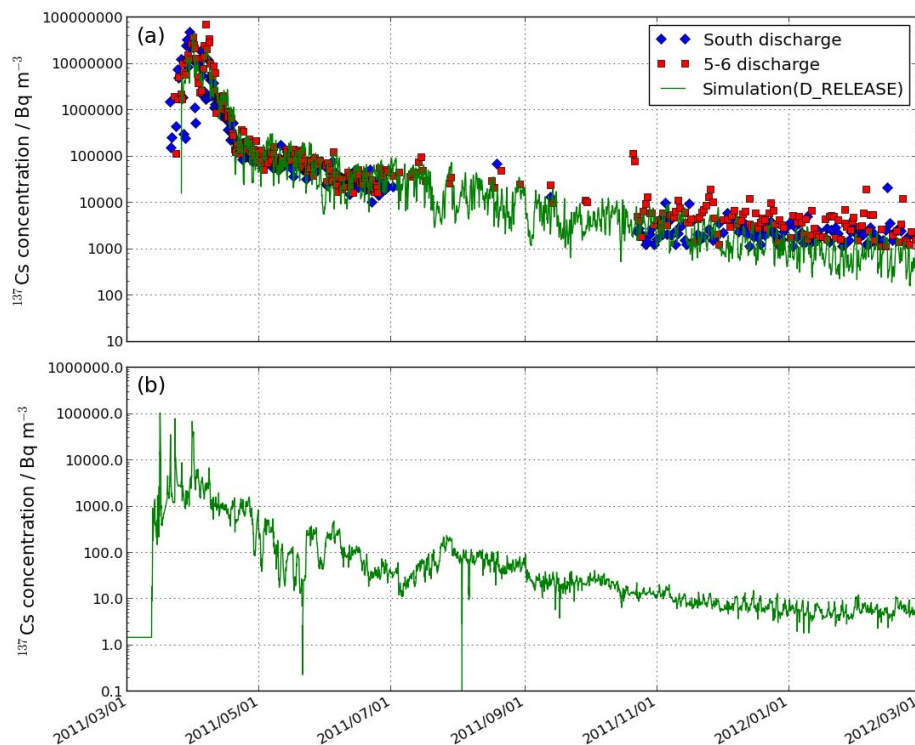


**Fig. 10.** (a) Measured  $^{137}\text{Cs}$  activities ( $\text{Bq m}^{-3}$ ) at the 5–6 (north) and south discharge canals near the 1F NPP and simulated  $^{137}\text{Cs}$  activities (D\_RELEASE scenario) in a grid adjacent to the 1F NPP site. (b) Difference of activities between the ALL and D\_RELEASE scenarios.

## One-year, regional-scale simulation of $^{137}\text{Cs}$ radioactivity in the ocean

D. Tsumune et al.

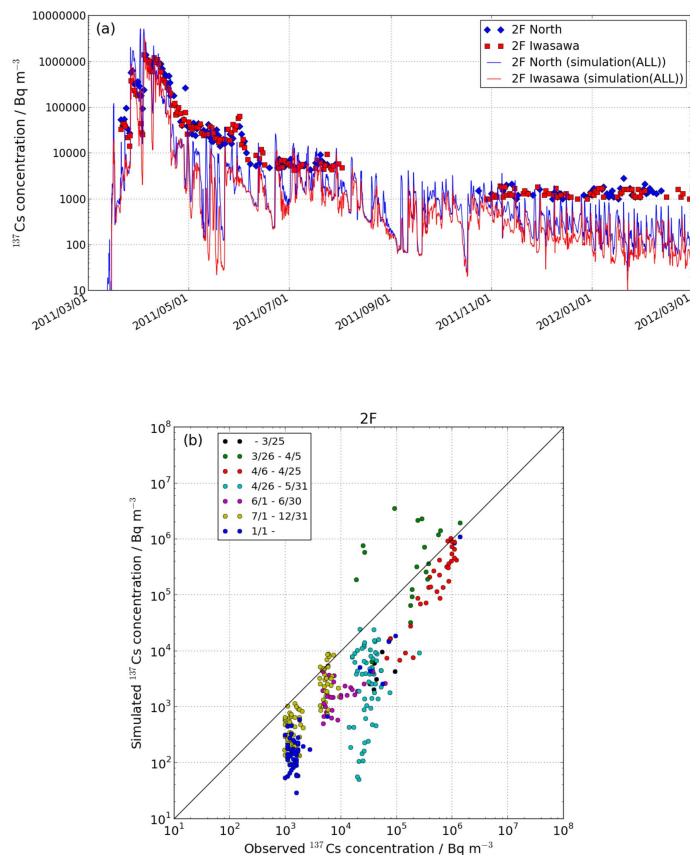


**Fig. 11.** (a) Measured  $^{137}\text{Cs}$  activities ( $\text{Bq m}^{-3}$ ) at the 2F north discharge canal (10 km south of the 1F NPP site) and offshore of Iwasawa (16 km south of the 1F NPP site) and simulated  $^{137}\text{Cs}$  activities (ALL scenario). (b) Scatter plot between daily mean measured and simulated activities.

Title Page

Abstract

Introduction

Conclusions

References

Tables

Figures

◀

▶

◀

▶

Back

Close

Full Screen / Esc

Printer-friendly Version

Interactive Discussion

## One-year, regional-scale simulation of $^{137}\text{Cs}$ radioactivity in the ocean

D. Tsumune et al.

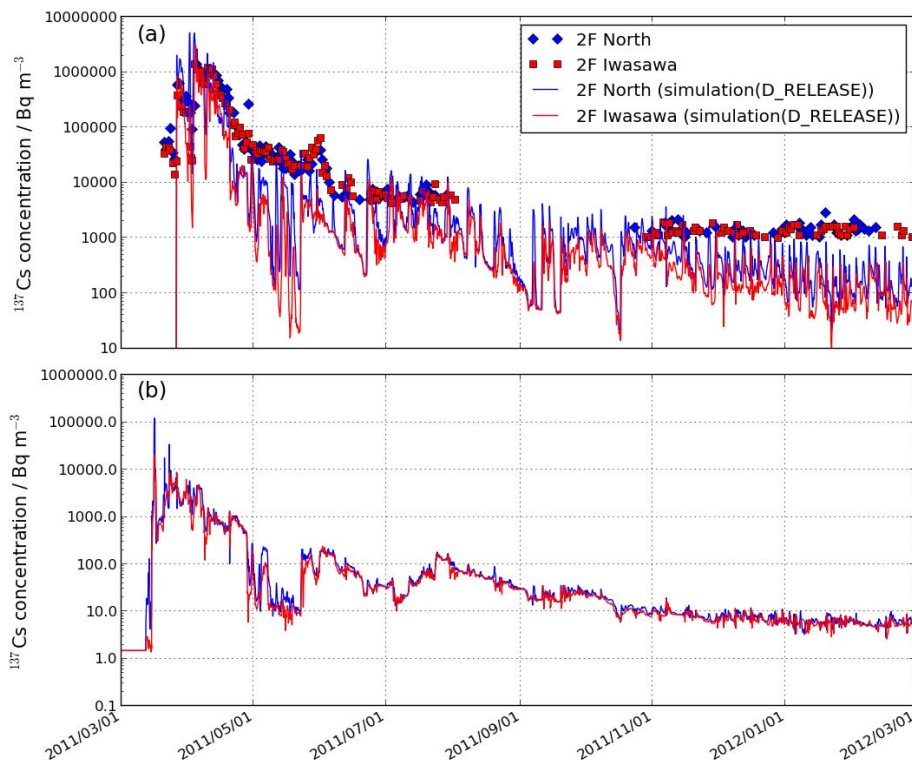


**Fig. 12.** (a) Measured  $^{137}\text{Cs}$  activities ( $\text{Bq m}^{-3}$ ) at the 2F north discharge canal (10 km south of the 1F NPP site) and off shore of Iwasawa (16 km south of the 1F NPP site) and simulated  $^{137}\text{Cs}$  activities (D\_RELEASE scenario). (b) Difference of activities between the ALL and D\_RELEASE scenarios.

[Title Page](#)
[Abstract](#)
[Introduction](#)
[Conclusions](#)
[References](#)
[Tables](#)
[Figures](#)
[◀](#)
[▶](#)
[◀](#)
[▶](#)
[Back](#)
[Close](#)
[Full Screen / Esc](#)
[Printer-friendly Version](#)
[Interactive Discussion](#)



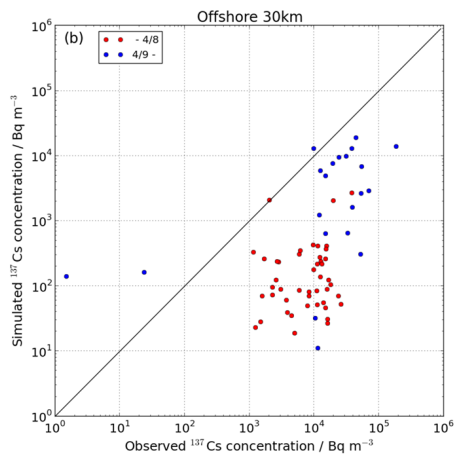
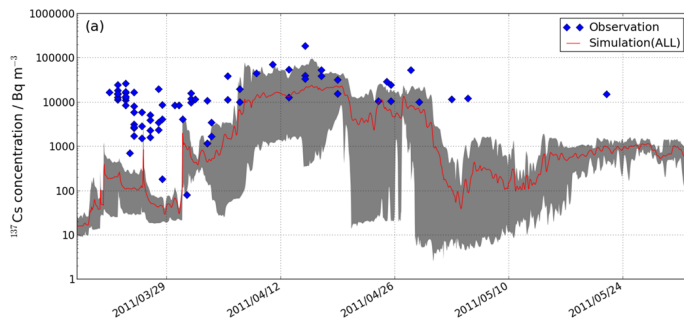


**Fig. 13. (a)** Measured  $^{137}\text{Cs}$  activities ( $\text{Bq m}^{-3}$ ) 30 km offshore in the surface water at sites 1–8 (Fig. S1) and simulated  $^{137}\text{Cs}$  activities at all sites (ALL scenario). **(b)** Scatter plot between daily mean measured and simulated activities.

One-year, regional-scale simulation of  $^{137}\text{Cs}$  radioactivity in the ocean

D. Tsumune et al.

Title Page

Abstract Introduction

Conclusions References

Tables Figures

◀ ▶

◀ ▶

Back Close

Full Screen / Esc

Printer-friendly Version

Interactive Discussion



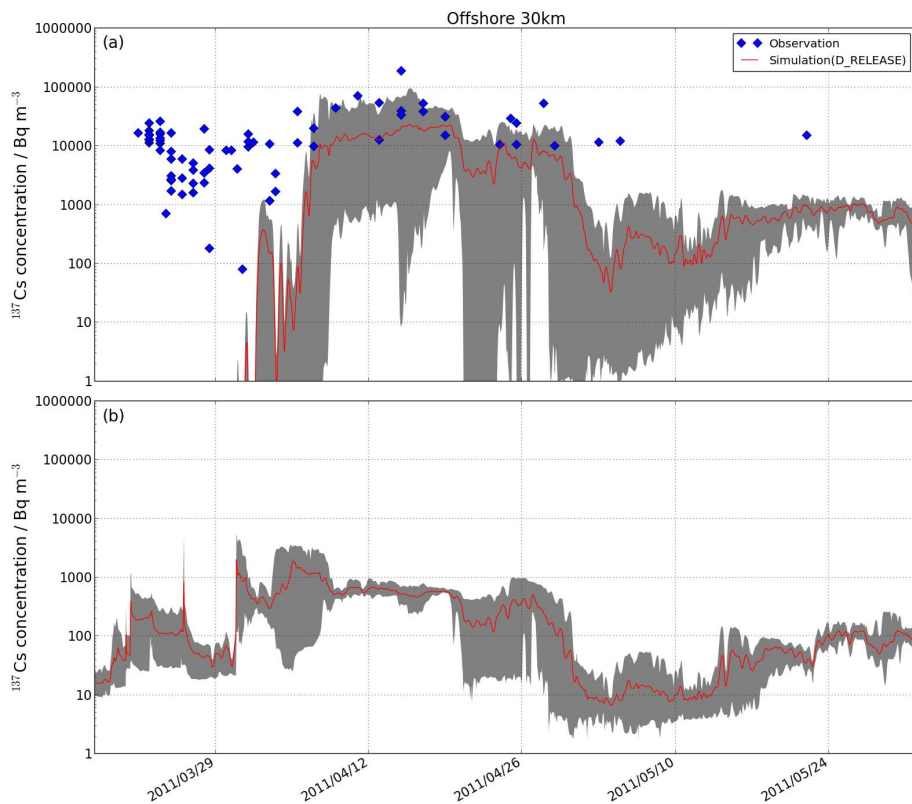


**Fig. 14.** (a) Measured  $^{137}\text{Cs}$  activities ( $\text{Bq m}^{-3}$ ) 30 km offshore and simulated  $^{137}\text{Cs}$  activities (D\_RELEASE scenario). (b) Difference of activities between ALL and D\_RELEASE scenarios.

One-year, regional-scale simulation of  $^{137}\text{Cs}$  radioactivity in the ocean

D. Tsumune et al.

Title Page

Abstract Introduction

Conclusions References

Tables Figures

◀ ▶

◀ ▶

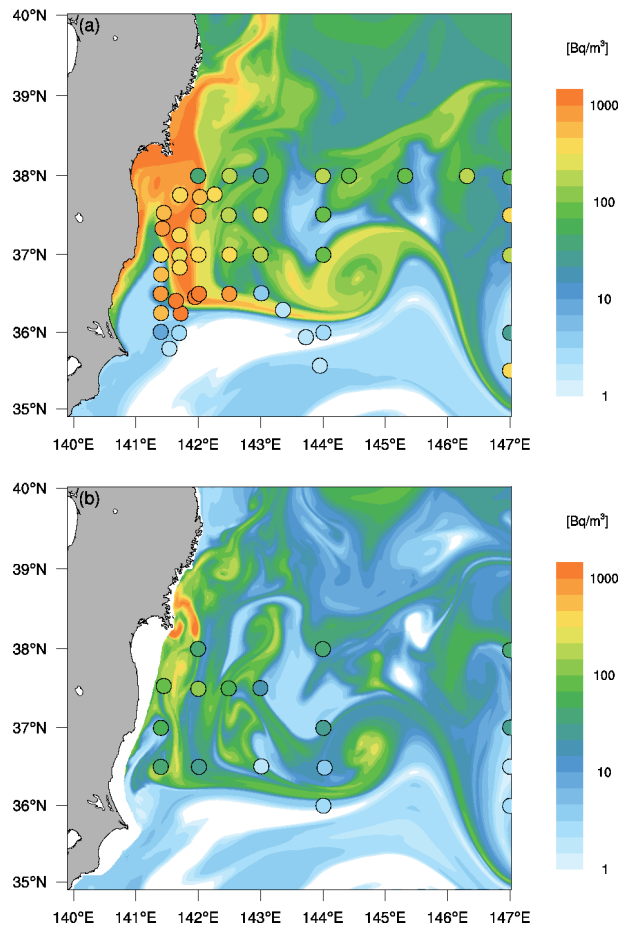
Back Close

Full Screen / Esc

Printer-friendly Version

Interactive Discussion

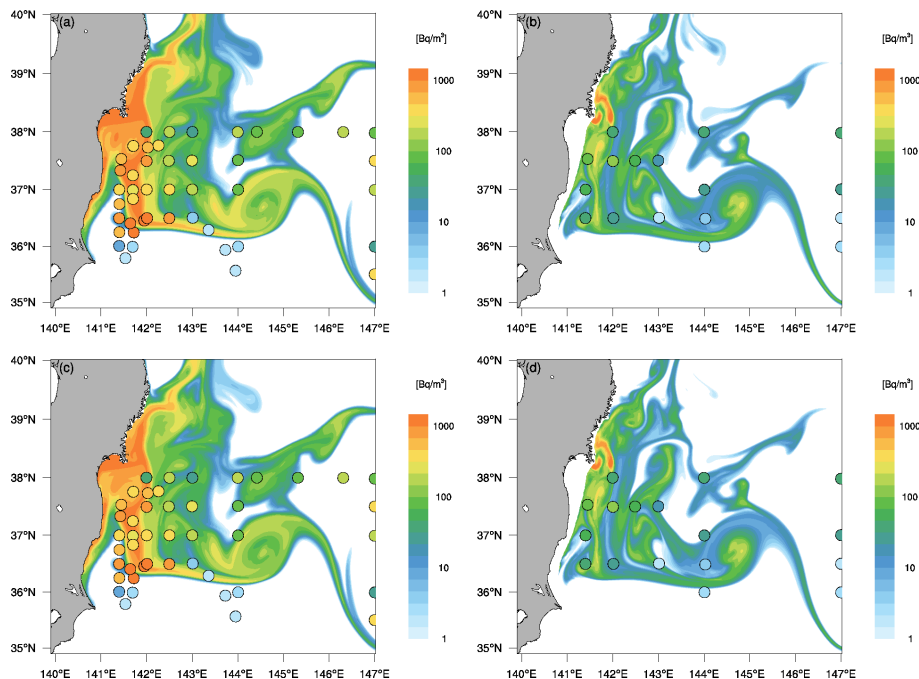




**Fig. 15.** (a) Simulated  $^{137}\text{Cs}$  activities ( $\text{Bq m}^{-3}$ ) in surface waters (ALL scenario) and (b) at a depth of 100 m on 15 June 2011 and measurements from 3–18 June 2011 (Buessler et al., 2012).

# One-year, regional-scale simulation of $^{137}\text{Cs}$ radioactivity in the ocean

D. Tsumune et al.

[Title Page](#)[Abstract](#)[Introduction](#)[Conclusions](#)[References](#)[Tables](#)[Figures](#)[⏪](#)[⏩](#)[◀](#)[▶](#)[Back](#)[Close](#)[Full Screen / Esc](#)[Printer-friendly Version](#)[Interactive Discussion](#)

**Fig. 16.**  $^{137}\text{Cs}$  activities ( $\text{Bq m}^{-3}$ ) simulated in the NO\_INFLOW scenario on 15 June 2011 **(a)** in surface waters and **(b)** at a depth of 100 m and measurements from 3–18 June 2011 (Buessler et al., 2012).  $^{137}\text{Cs}$  activities simulated in the D\_RELEASE scenario **(c)** in surface waters and **(d)** at a depth of 100 m.

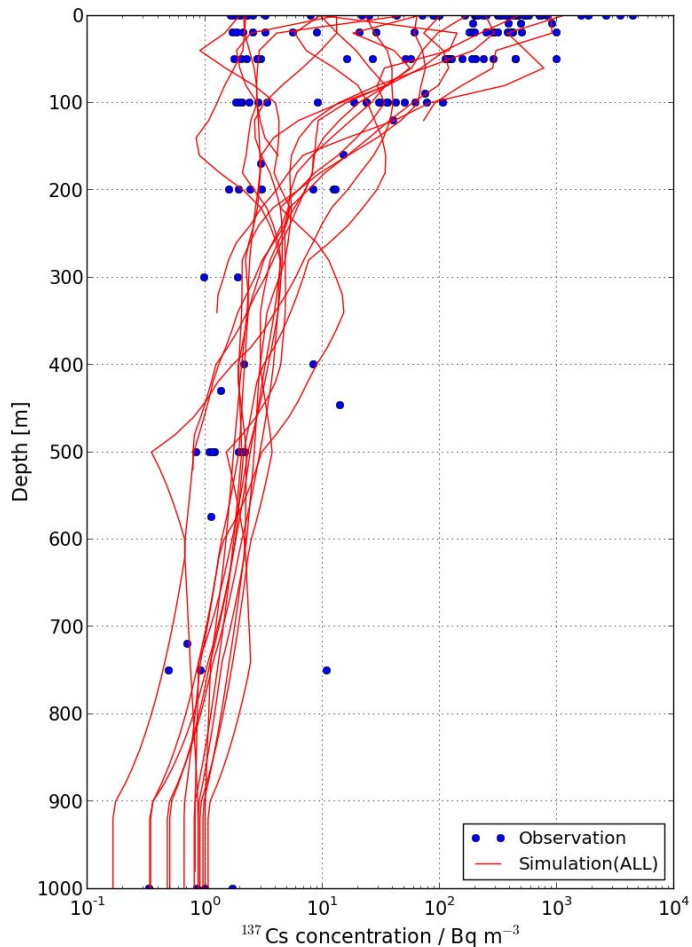


**Fig. 17.** Measured and simulated (ALL scenario) vertical profiles of  $^{137}\text{Cs}$  activities ( $\text{Bq m}^{-3}$ ) in the area of the KOK cruise (Buesseler et al., 2012).

**One-year, regional-scale simulation of  $^{137}\text{Cs}$  radioactivity in the ocean**

D. Tsumune et al.

[Title Page](#)

[Abstract](#)   [Introduction](#)

[Conclusions](#)   [References](#)

[Tables](#)   [Figures](#)

[◀](#)   [▶](#)

[◀](#)   [▶](#)

[Back](#)   [Close](#)

[Full Screen / Esc](#)

[Printer-friendly Version](#)

[Interactive Discussion](#)



## One-year, regional-scale simulation of $^{137}\text{Cs}$ radioactivity in the ocean

D. Tsumune et al.

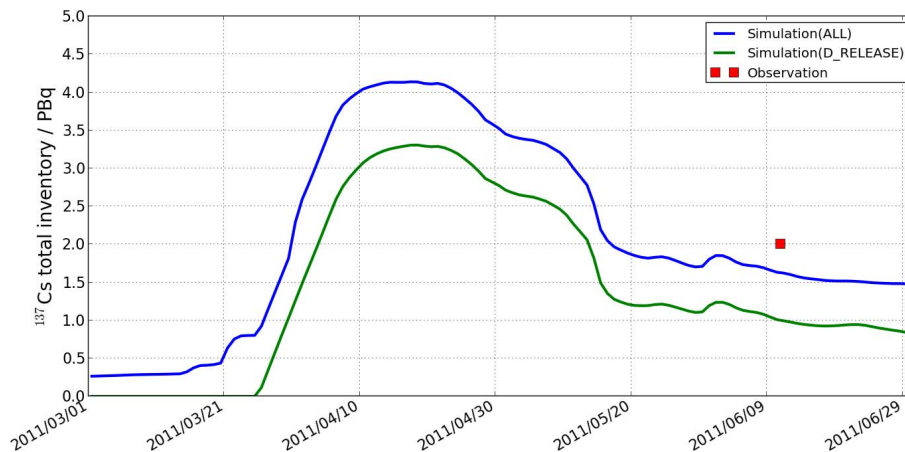


**Fig. 18.** Simulated total inventories (PBq) in the area of the KOK cruise by ALL and D.RELEASE scenarios.

[Title Page](#)[Abstract](#)[Introduction](#)[Conclusions](#)[References](#)[Tables](#)[Figures](#)[◀](#)[▶](#)[◀](#)[▶](#)[Back](#)[Close](#)[Full Screen / Esc](#)[Printer-friendly Version](#)[Interactive Discussion](#)

## One-year, regional-scale simulation of $^{137}\text{Cs}$ radioactivity in the ocean

D. Tsumune et al.

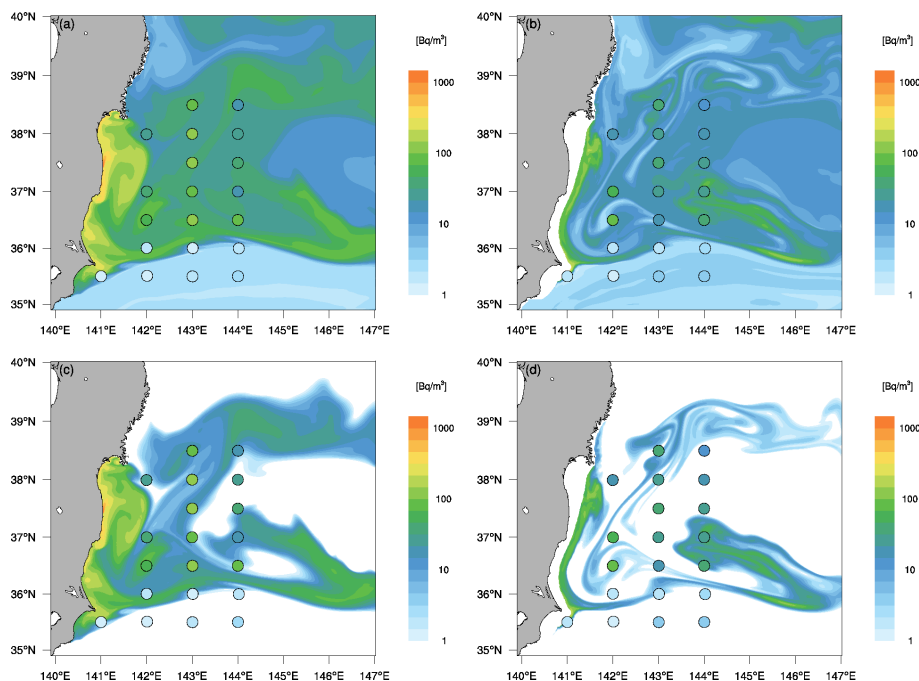


**Fig. 19.** Simulated  $^{137}\text{Cs}$  activities ( $\text{Bq m}^{-3}$ ) (ALL case) on 25 August 2011 **(a)** in surface waters and **(b)** at a depth of 100 m and measurements from 23–27 August 2011. Simulated  $^{137}\text{Cs}$  activities (D-RELEASE scenario) **(c)** in surface waters and **(d)** at a depth of 100 m.

Title Page

Abstract

Introduction

Conclusions

References

Tables

Figures

◀

▶

◀

▶

Back

Close

Full Screen / Esc

Printer-friendly Version

Interactive Discussion

# One-year, regional-scale simulation of $^{137}\text{Cs}$ radioactivity in the ocean

D. Tsumune et al.

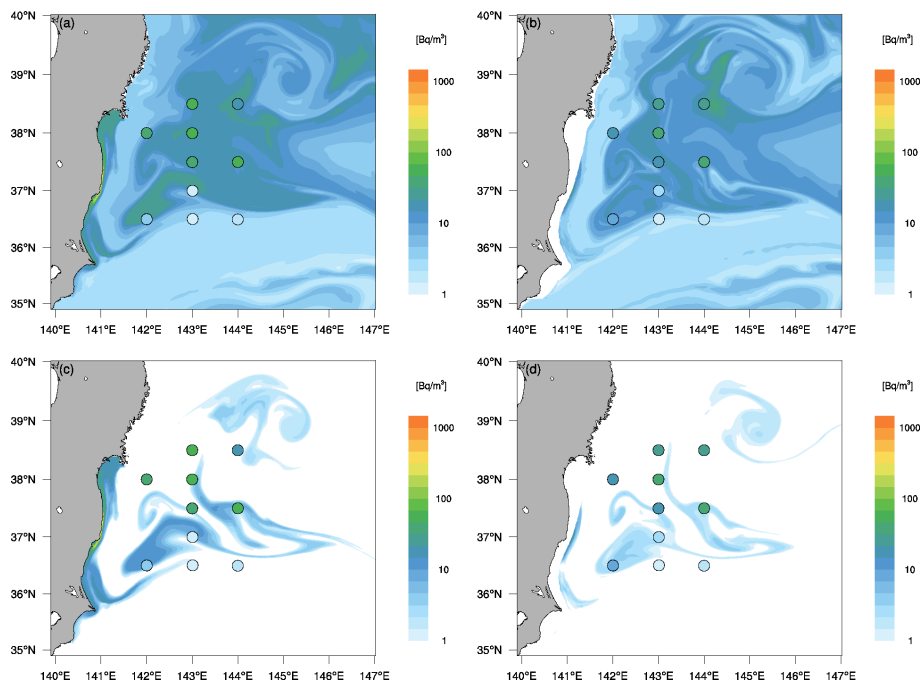


**Fig. 20.** Simulated  $^{137}\text{Cs}$  activities ( $\text{Bq m}^{-3}$ ) (ALL scenario) on 2 December 2011 **(a)** in surface waters and **(b)** at a depth of 100 m and observations from 30 November to 2 December 2011. Simulated  $^{137}\text{Cs}$  activities (D.RELEASE scenario) **(c)** in surface waters and **(d)** at a depth of 100 m.

Title Page

Abstract

Introduction

Conclusions

References

Tables

Figures

⏪

⏩

◀

▶

Back

Close

Full Screen / Esc

Printer-friendly Version

Interactive Discussion